

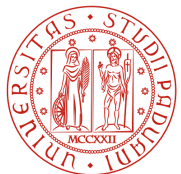
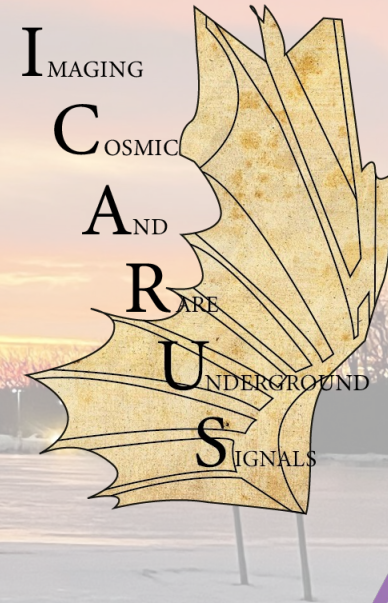
# First results from the search for $\nu_\mu$ disappearance with ICARUS

Maria Artero Pons Università degli Studi di Padova and INFN Padova

On behalf of the ICARUS Collaboration

Rencontres de Moriond – EW session

La Thuile, 15-22 March 2026



UNIVERSITÀ  
DEGLI STUDI  
DI PADOVA

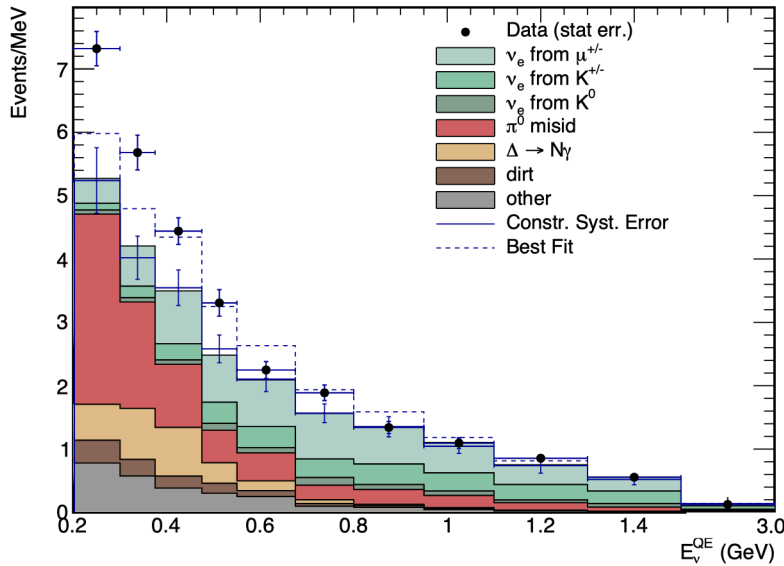


[maria.arteropons@pd.infn.it](mailto:maria.arteropons@pd.infn.it)

# The sterile neutrino puzzle

- Several anomalies collected so far hinting to additional  $\nu$  states driving oscillations with  $\Delta m^2 \sim eV^2$

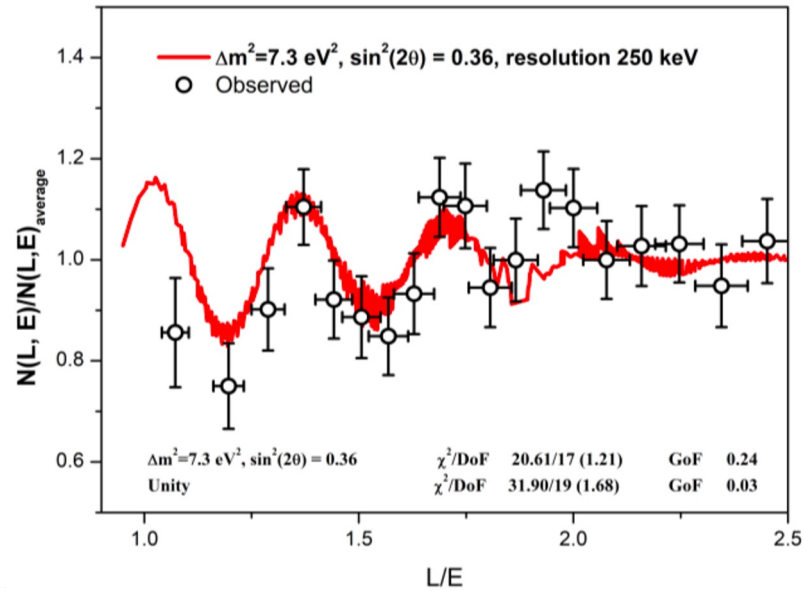
Low energy excess of  $\nu_e$  like events in [LSND](#) and [MiniBooNE](#)



[Phys. Rev. D 103, 052002](#)

6.1 $\sigma$  combined significance for the excess observed in LSND and MiniBooNE

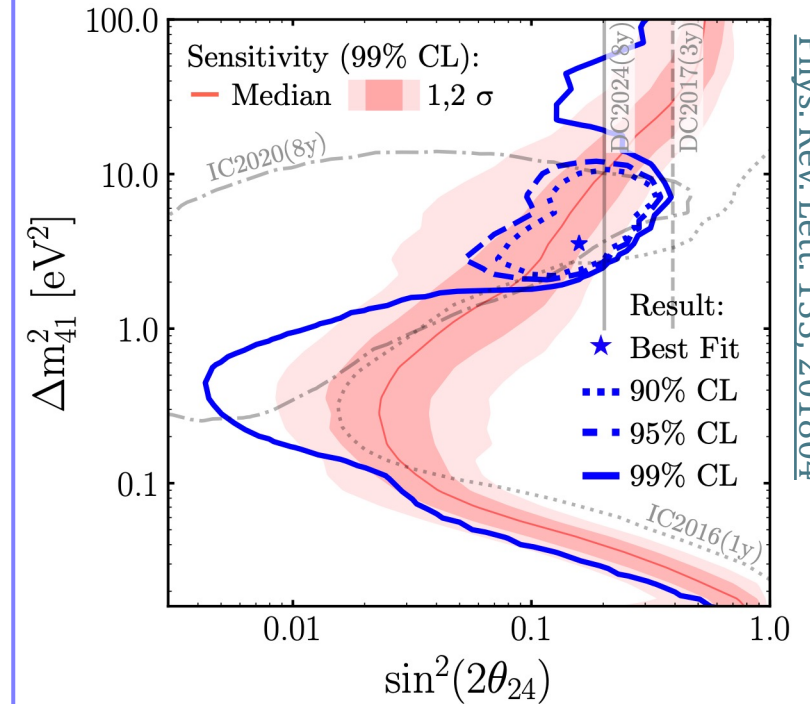
Reactor  $\bar{\nu}_e$  disappearance signal by Neutrino-4



[arXiv:2302.09958](#)

Signal at 5.8 $\sigma$  CL when results are combined with other experiments

$\nu_\mu$  disappearance signal by IceCube

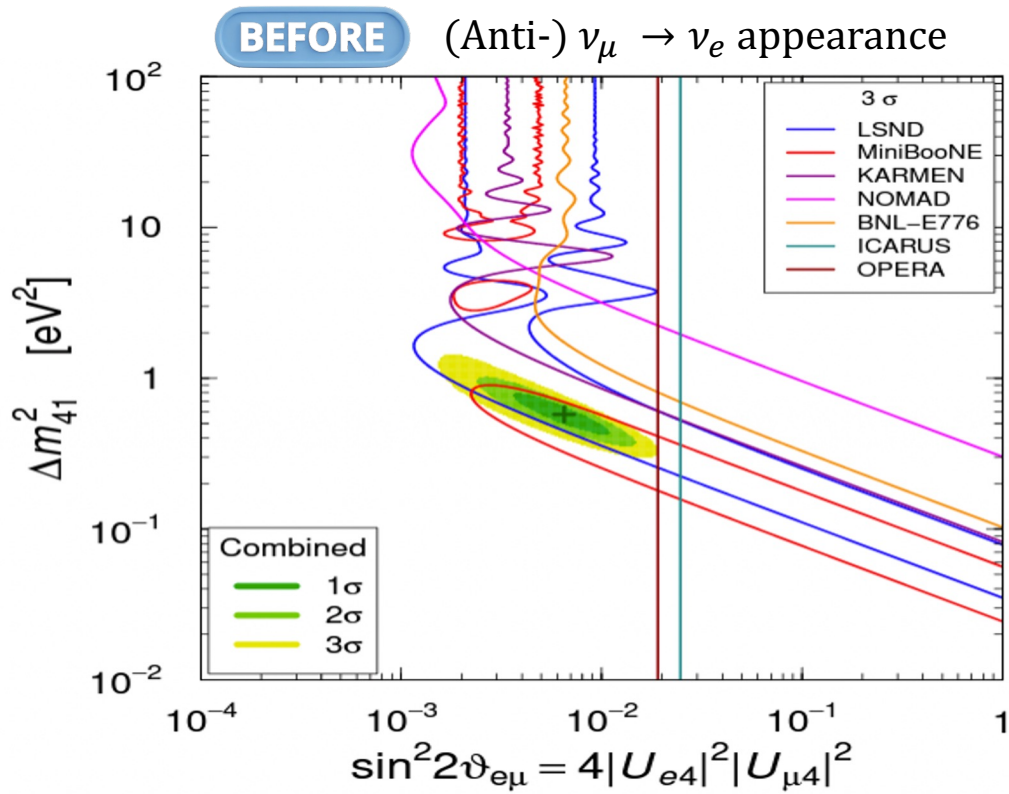


[Phys. Rev. Lett. 133, 201804](#)

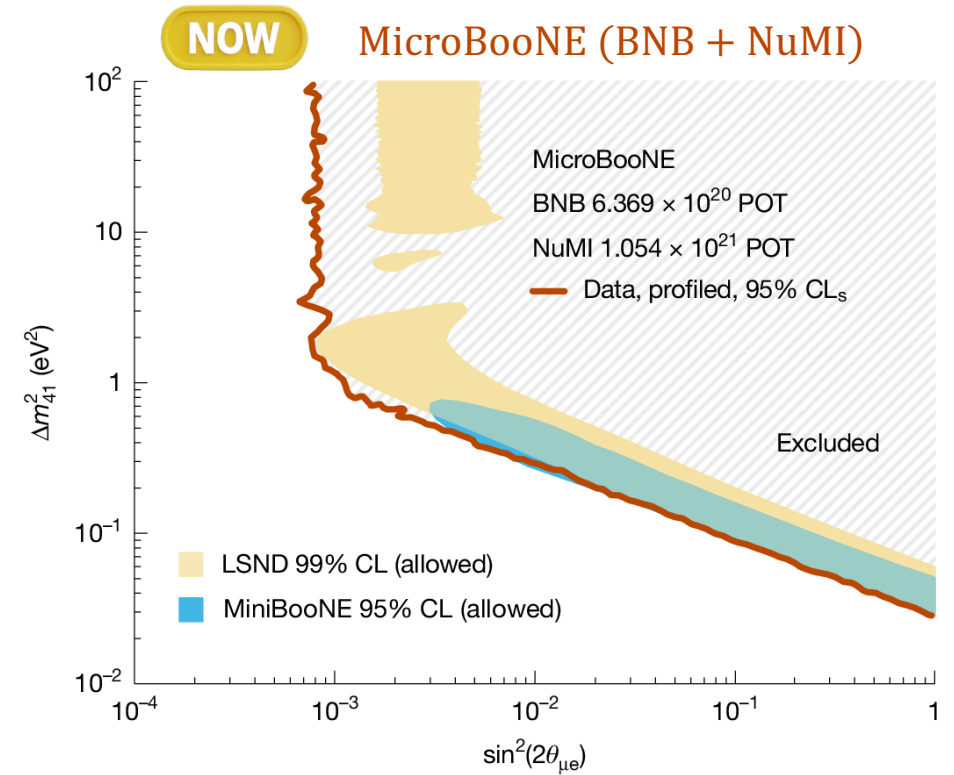
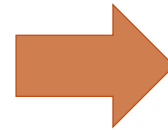
Closed contour observed at 95% CL using atmospheric neutrinos

# Current experimental status

- LSND and MiniBooNE allowed regions largely ruled out by MicroBooNE at 95% CL using  $\nu_e$  and  $\nu_\mu$  from two beams



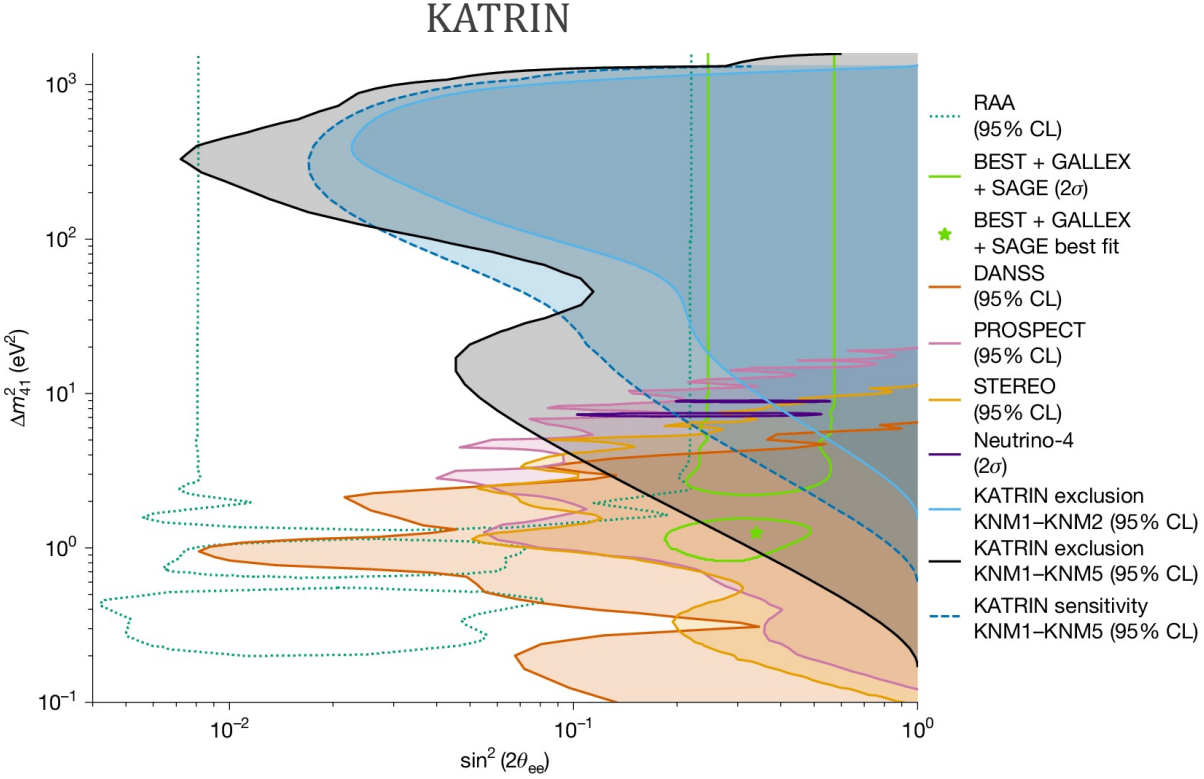
[arXiv:2106.05913](https://arxiv.org/abs/2106.05913)



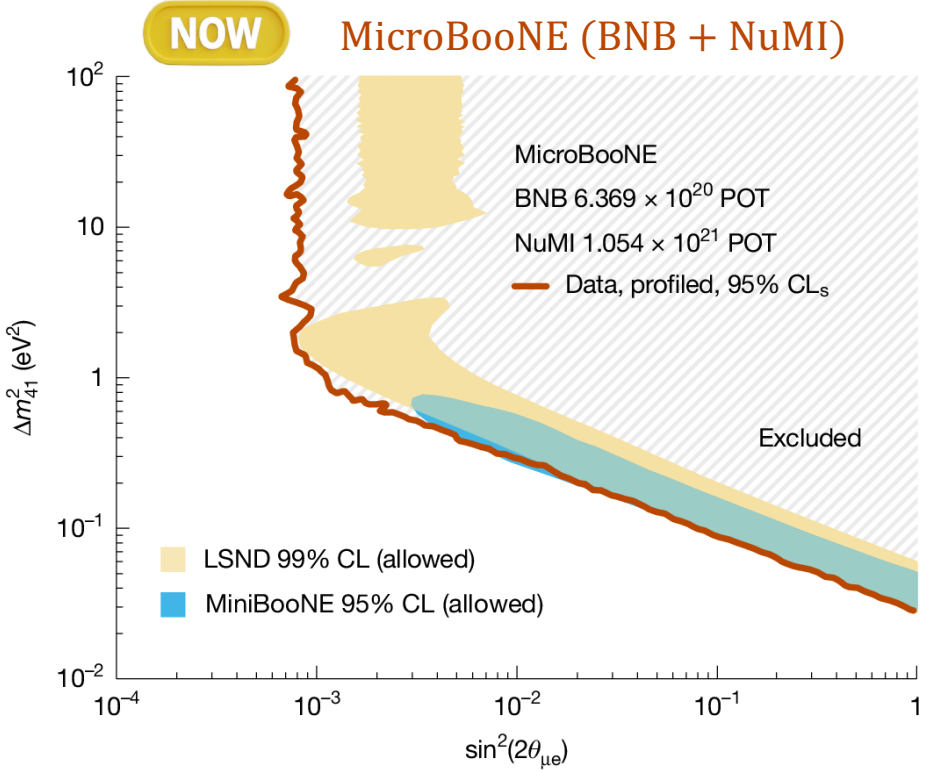
[Nature 648, 64–69 \(2025\)](https://doi.org/10.1038/s41586-025-0450-4)

# Current experimental status

- LSND and MiniBooNE allowed regions largely ruled out by MicroBooNE at 95% CL using  $\nu_e$  and  $\nu_\mu$  from two beams
- $\beta$  – decay experiment KATRIN also ruled out much of the favoured  $\theta_{ee}$  parameter space at 95% CL



[Nature 648, 70–75 \(2025\)](#)



[Nature 648, 64–69 \(2025\)](#)

# The sterile neutrino puzzle



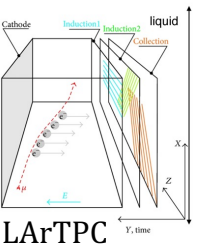
Tension between appearance and disappearance results in global constraint plots



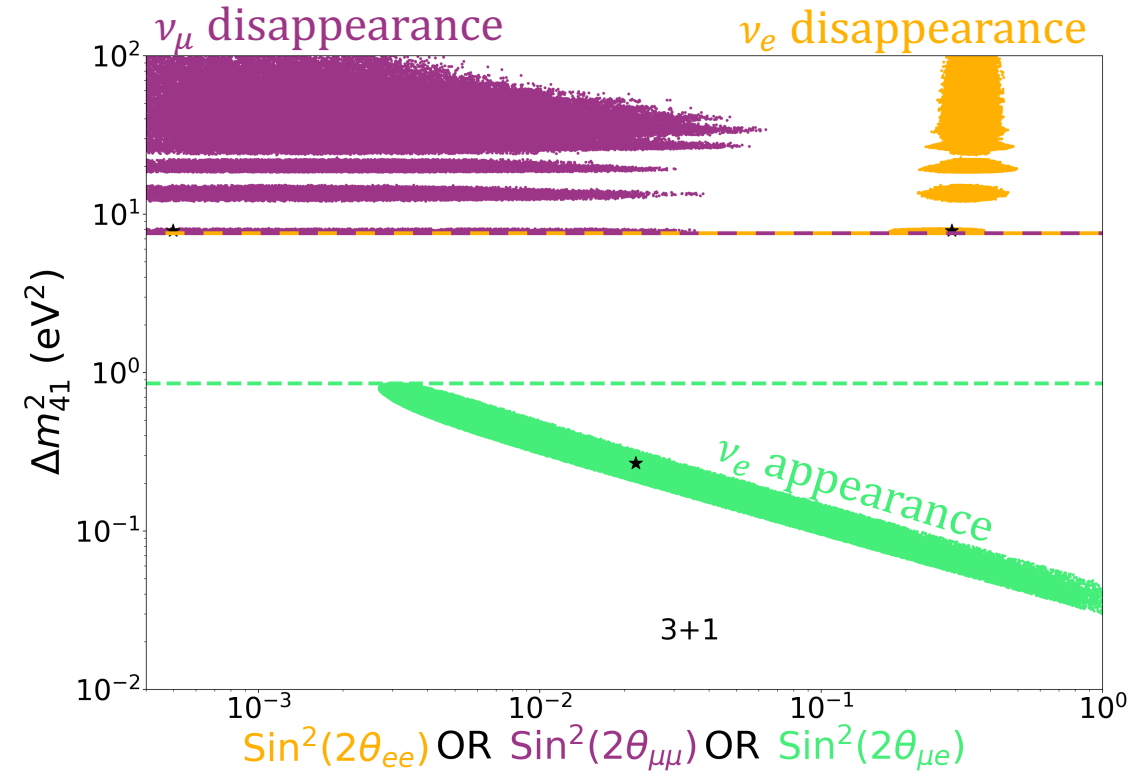
Measure both channels with the same experiment



The Short-Baseline Neutrino program is searching for sterile neutrinos at  $\sim eV^2$  mass scale

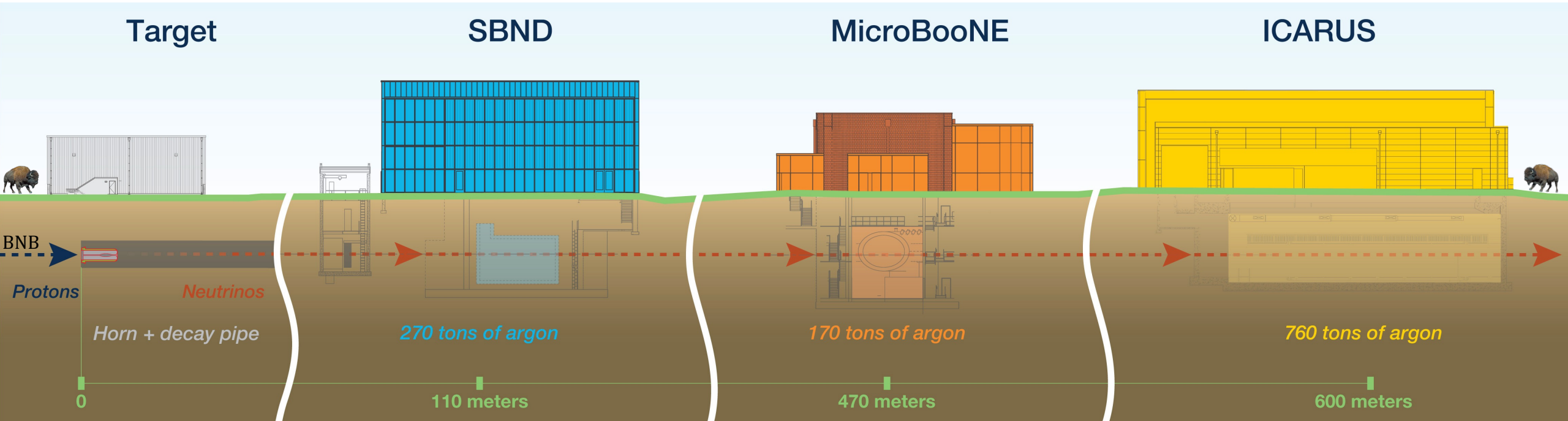


LAr Time Projection Chambers (LArTPC) @ Fermilab sampling the same  $\nu$  beam at different distances



[J. High Energ. Phys. 2023, 58 \(2023\)](#)

# The Short-Baseline Neutrino program



- Shared detector technology, nuclear target and beam to reduce the systematic uncertainties to % level



Flux and  $\nu - \text{Ar}$  cross section constraints from the near detector

Taking data since 2024

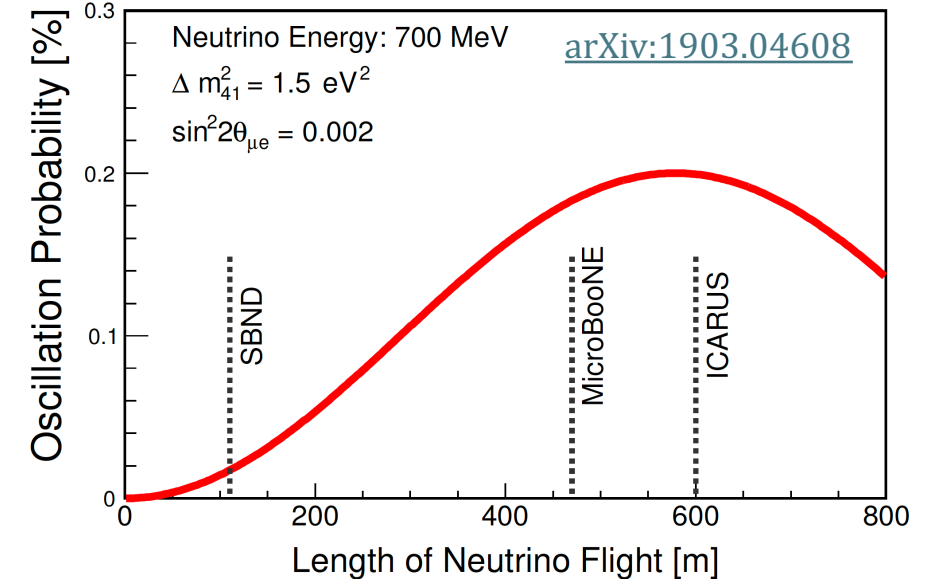
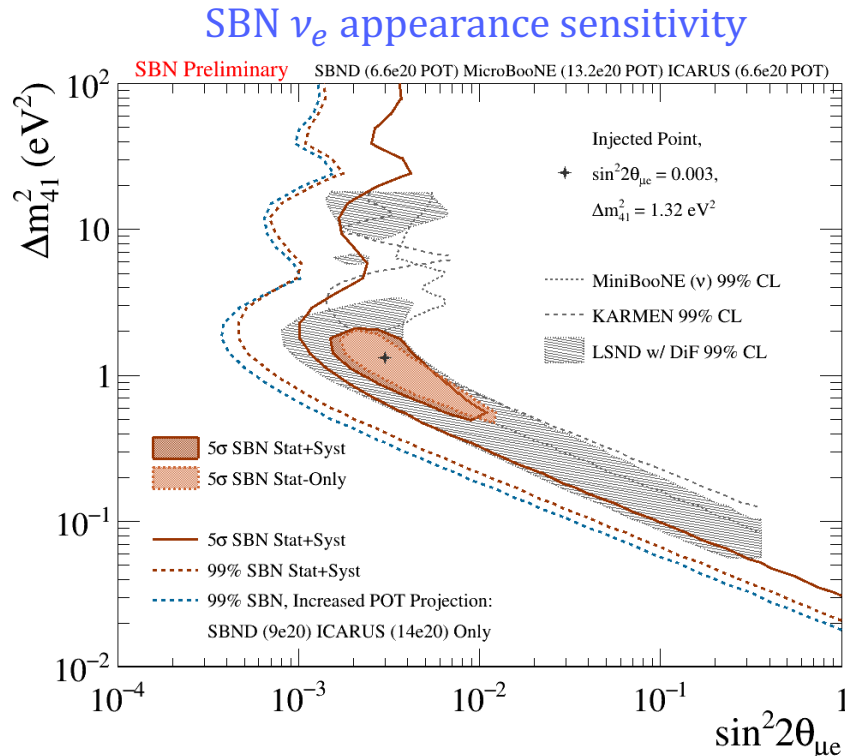
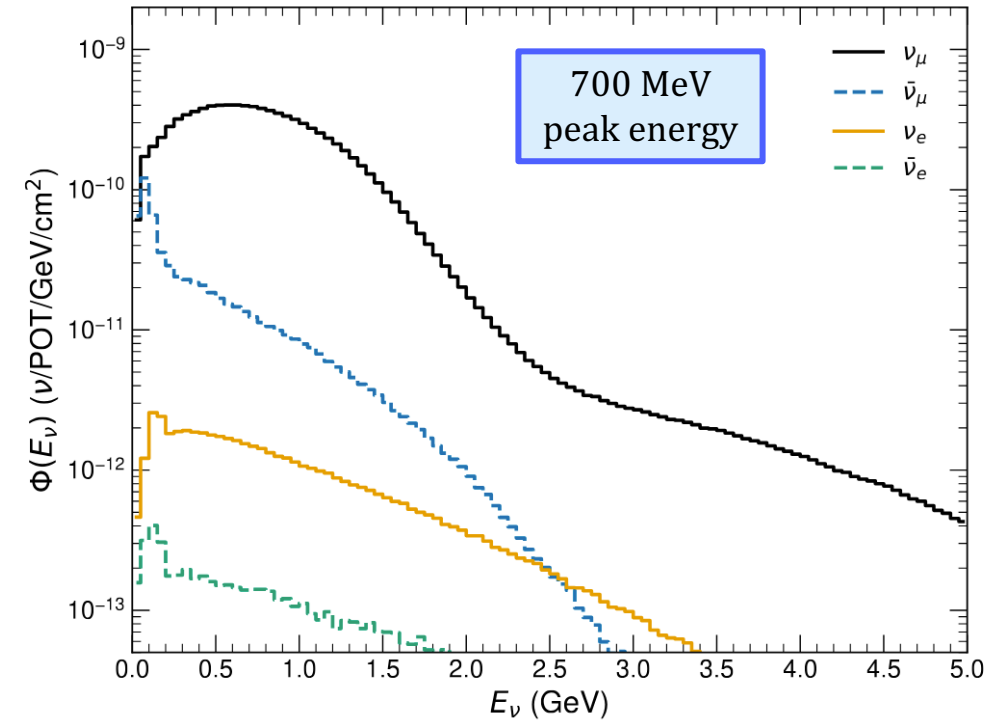
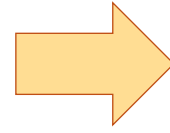


Oscillated neutrino spectrum measurement at the far detector

Taking data since 2022

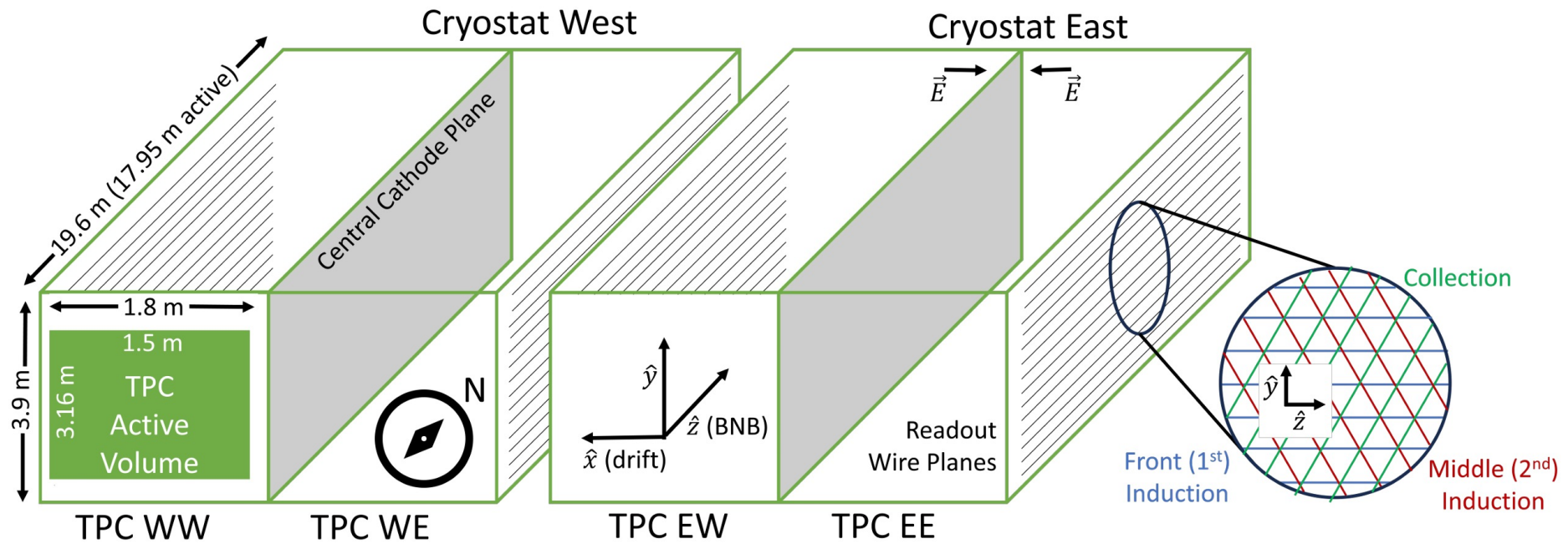
# Booster Neutrino Beam

- BNB is a dominated  $\nu_\mu$ -beam, able to produce  $\nu$  and  $\bar{\nu}$  beams with low  $\nu_e$  contamination (0.5%)
- Sensitive search in the  $\nu_\mu$  disappearance &  $\nu_e$  appearance channels



# ICARUS LArTPC

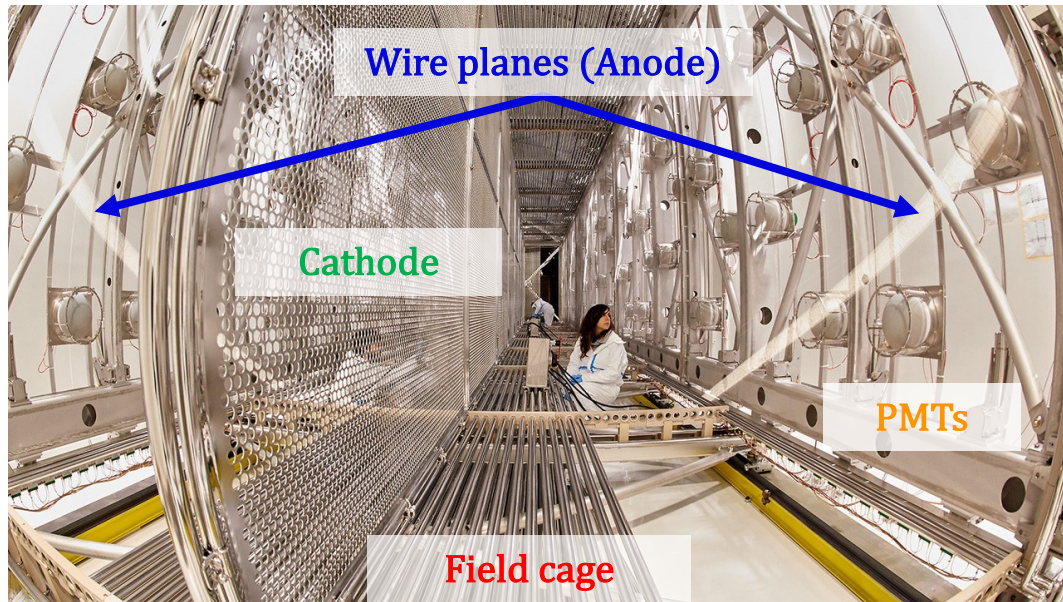
- ICARUS T600 is the first large scale LArTPC



- 2 Identical cryostats with 4 TPCs
- Total active mass 476 ton
- 3 readout wire planes per anode at 0 and  $\pm 60^\circ$
- 500 V/cm  $\vec{E}$  field, with 1.5 m drift length
- Warm front-end electronics

# ICARUS Detector Subsystems

See more details  
[Eur. Phys. J. C 83, 467 \(2023\)](#)



## Time Projection Chambers (TPC)

- ~ 54k channels at different orientations and 3 mm pitch

## Photon Detection System (PDS)

- 360 PMTs, TPB coated to detect scintillation light
- Event timing and triggering purposes



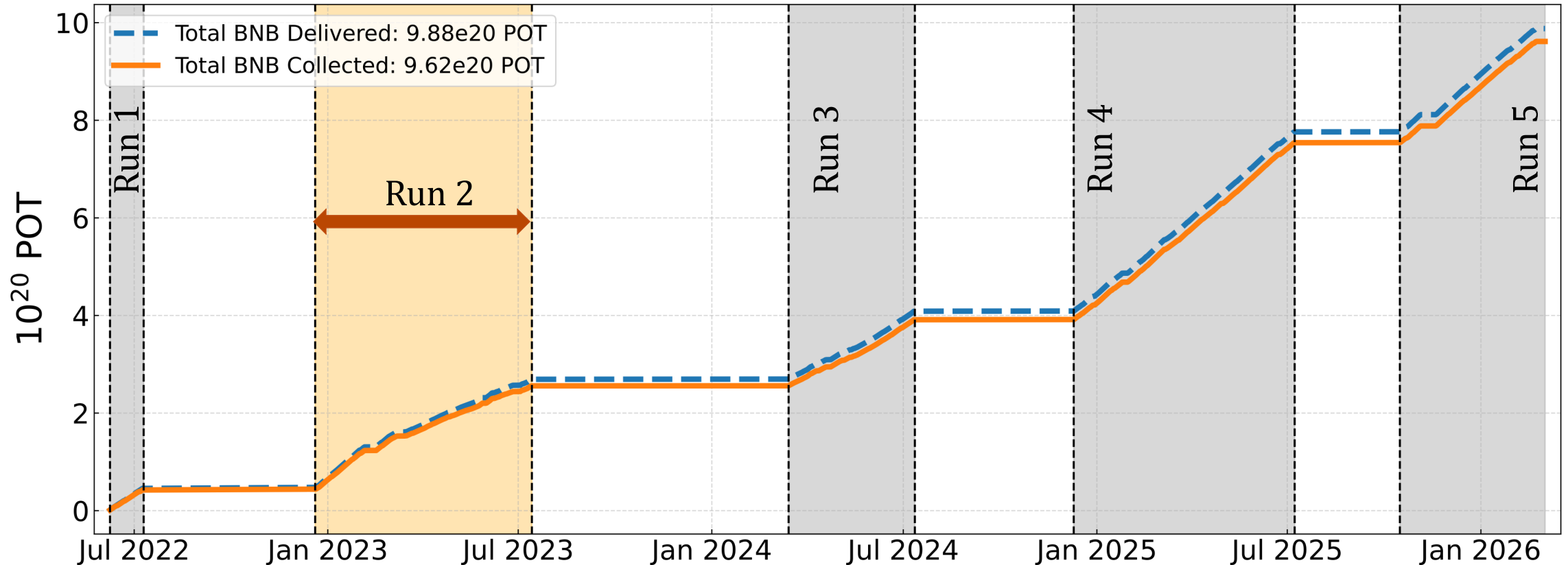
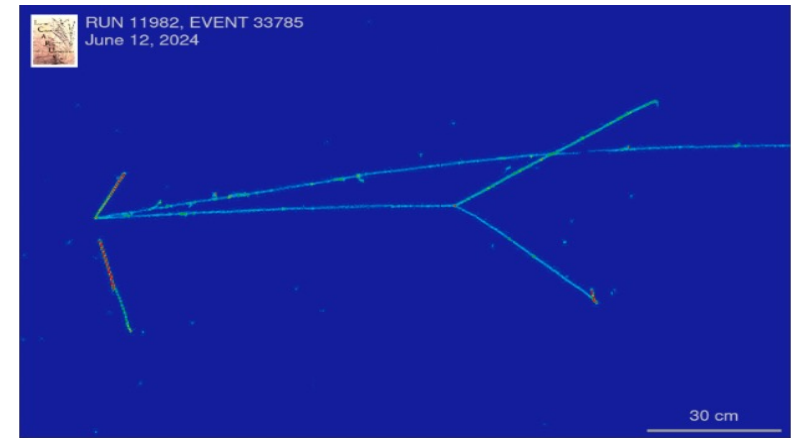
## Cosmic Ray rejection strategies

- Cosmic Ray Tagger (CRT): ~  $4\pi$  scintillator panels with SiPM readout for cosmic tagging
- Protected by ~ 2.85 m thick concrete overburden for external  $\gamma/n$  suppression

\*ICARUS operates at shallow depth

# ICARUS operation at FNAL

- Protons on target collected in the different ICARUS physics runs
- $\nu_\mu$  disappearance search uses **Run 2** data,  $\sim 2 \cdot 10^{20}$  POT in BNB
- Final exposure after beam and data quality cuts applied is  $1.6 \cdot 10^{20}$  POT

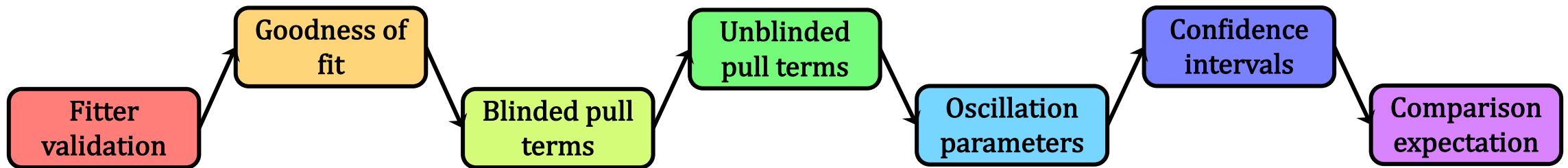


# First oscillation analysis

- Single detector  $\nu_\mu$  disappearance search
- **Systematics limited** analysis due to unconstrained systematics
- Crucial to the development of end-to-end analysis in view of SBN program
- Selection and systematics created with simulation and only 10% of Run 2



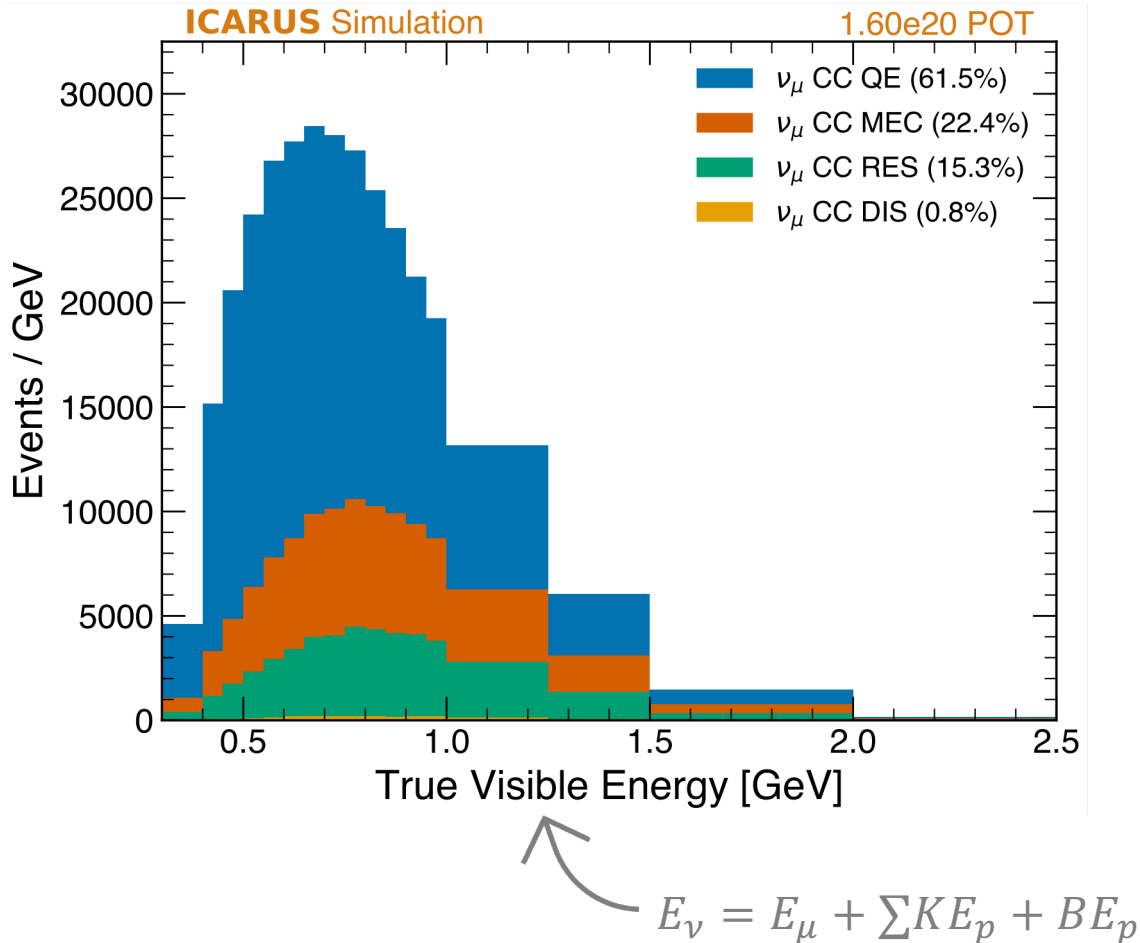
- New statistical analysis framework developed for SBN and tested exclusively with MC
- Staged **unblinding** fit to data, with results revealed only after thorough fit validation



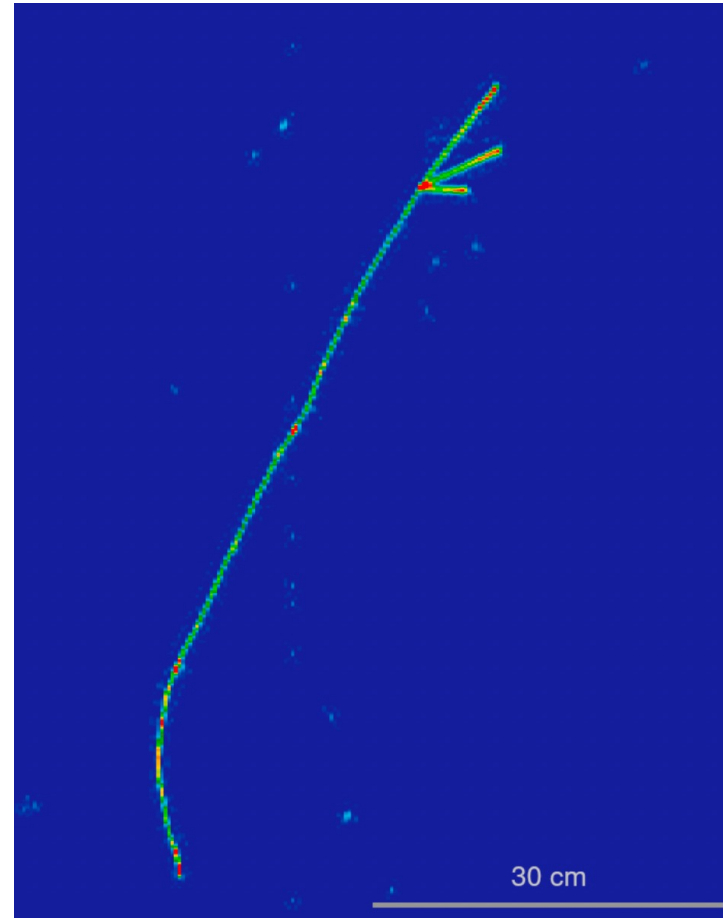


# Target sample

- $\nu_\mu$  CC contained interactions with only a muon and at least one proton in the final state ( $1\mu Np$ )

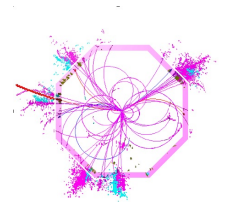


- Two independent reconstruction approaches



**SPINE**

Machine Learning  
with CNNs and GNNs



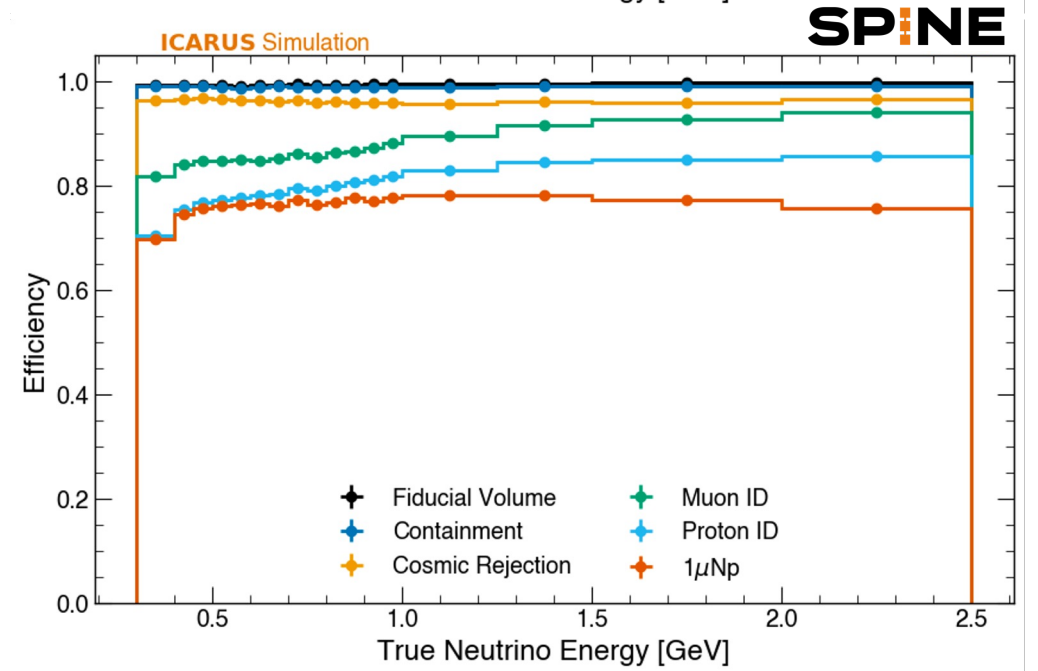
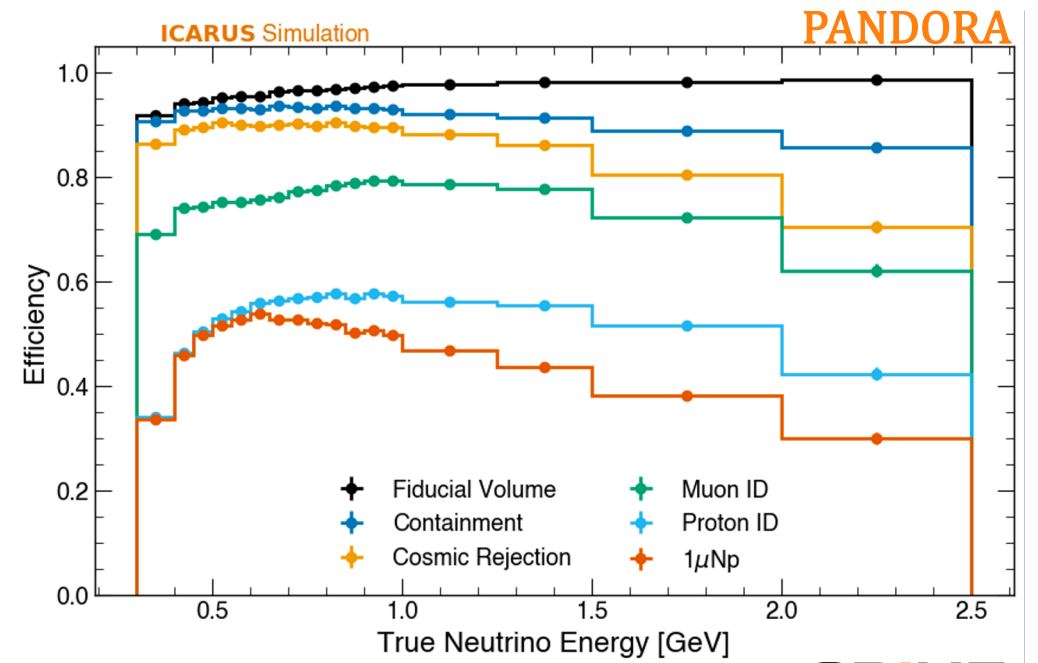
Pandora-based  
pattern recognition  
algorithm



# Event selection

- Fully contained  $\nu_\mu$  CC within fiducial volume
- Only one  $\mu$  with  $L_\mu > 50$  cm ( $p_\mu > 226$  MeV/c)
- At least a proton with  $E_{dep} > 50$  MeV
- No additional  $\gamma$  or  $\pi^\pm$  with  $E_{dep} > 25$  MeV
- Cosmic rejection based on charge, light and ...
  - + CRT (Pandora)
  - + beam timing (SPINE) information

	Purity	Efficiency
Pandora	81.5 %	48.5 %
SPINE	91.6 %	77.0 %



Quoted numbers with respect to target sample ( $1\mu Np$ ) and validated through visual scanning of the events

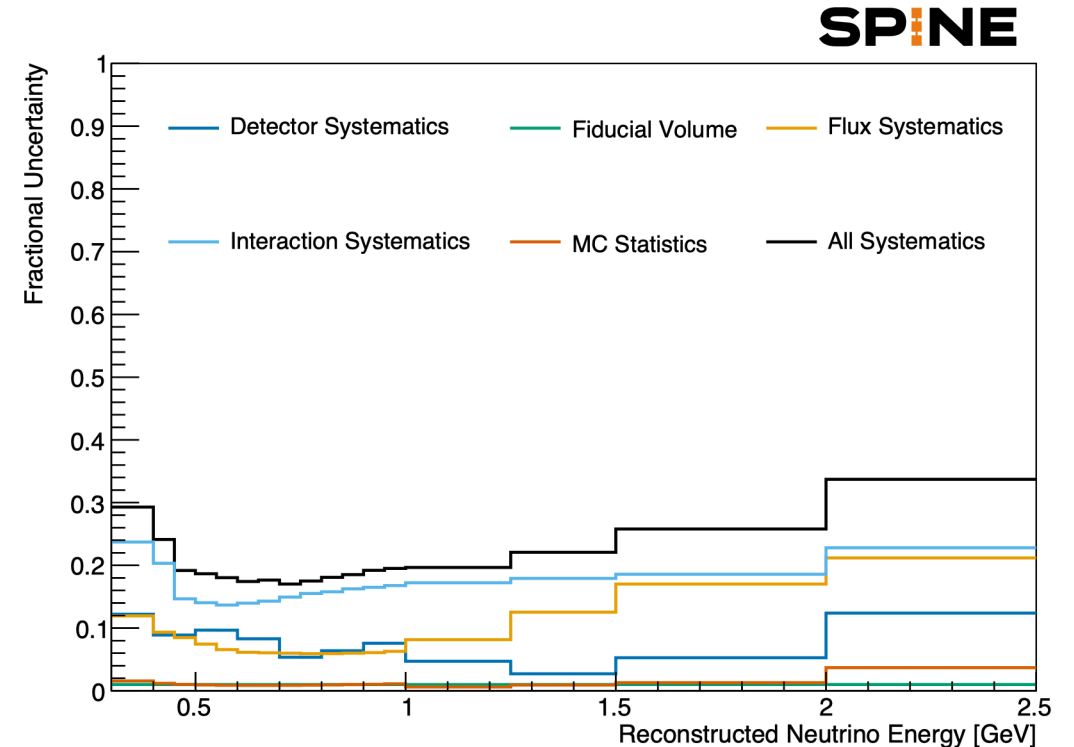
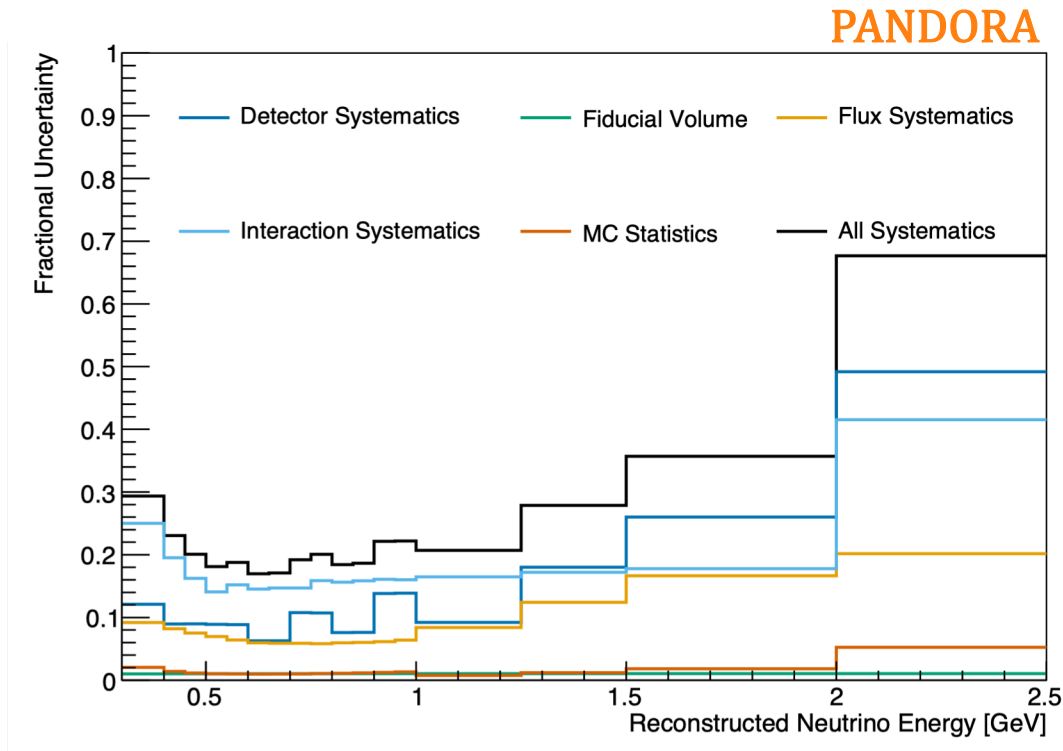
# Overall systematic uncertainties

- Full suite of systematics uncertainties. Evaluated by comparing nominal with shifted simulated samples



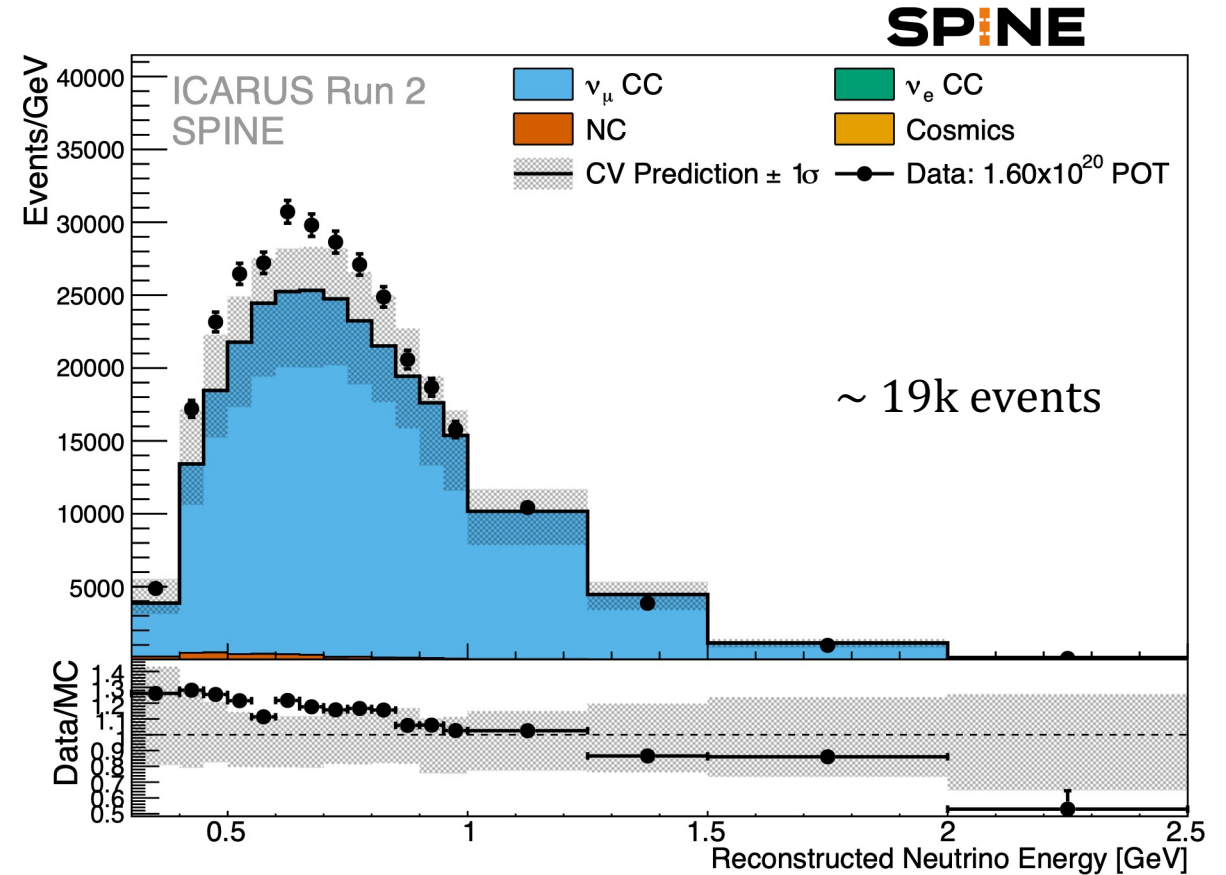
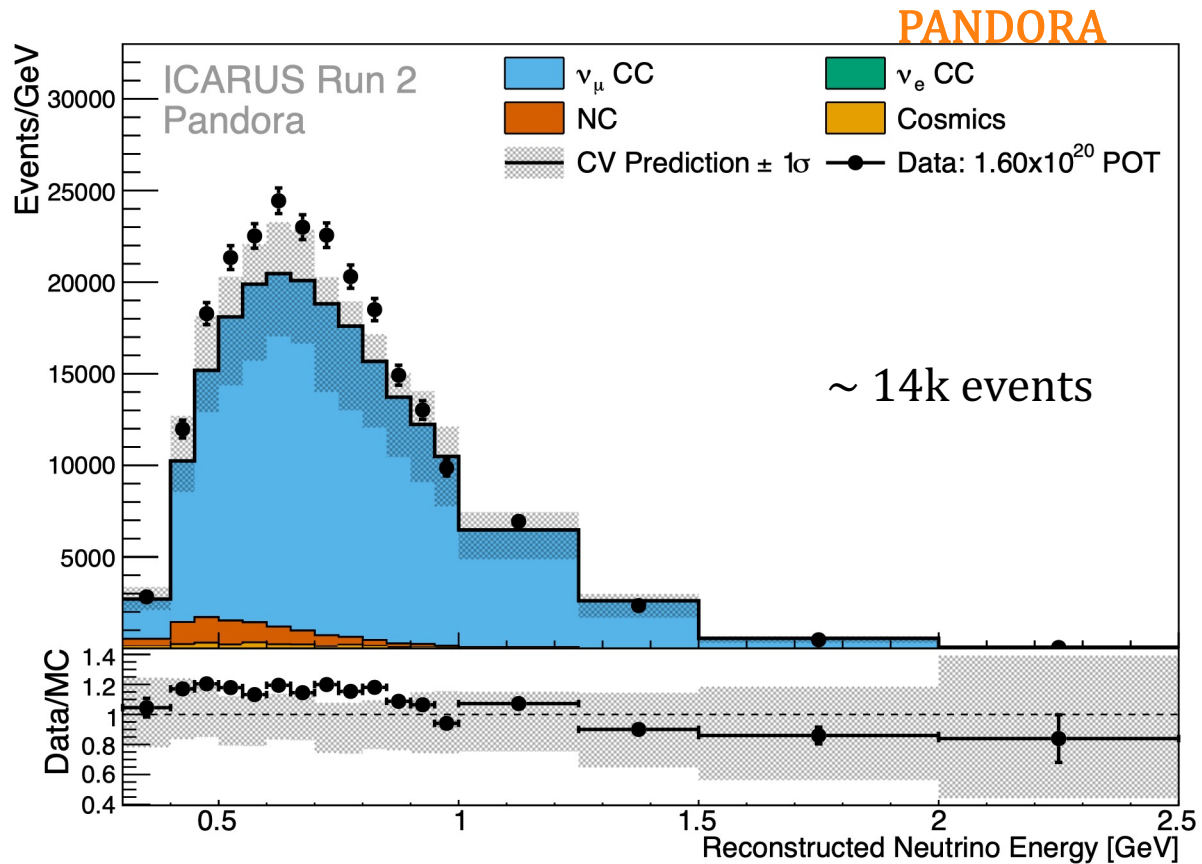
Including flux, cross section and detector uncertainties

- Future analyses will benefit from SBND data and improved simulation closely matching the data



# Data – Simulation comparison

- Data points are generally above the central value, expected given the interaction model used (GENIE AR23)
- Good shape agreement in both cases

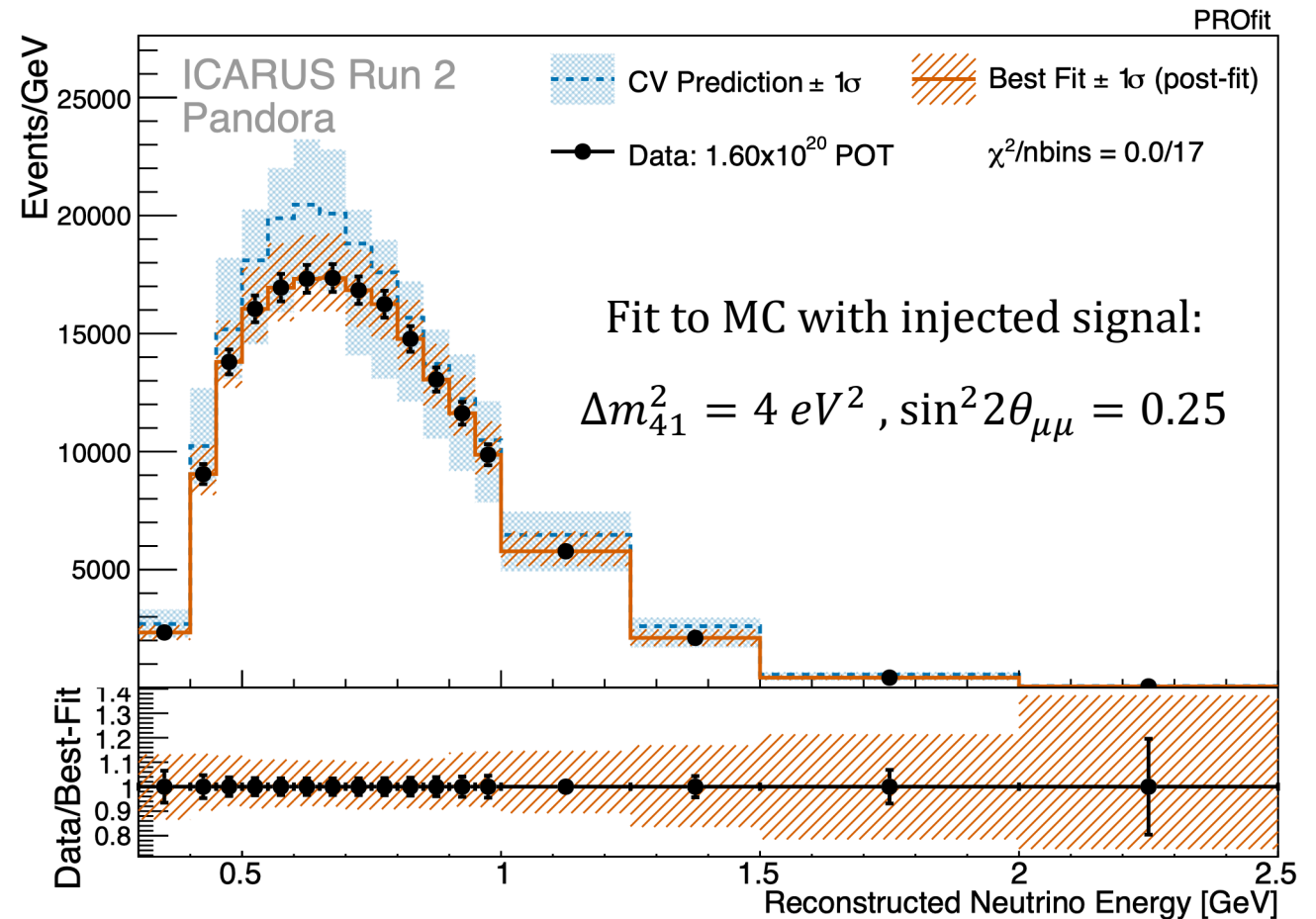


# Fitting and statistical analysis

- Brand new statistical analysis framework developed for SBN: PROfit

- Main features used in this analysis:

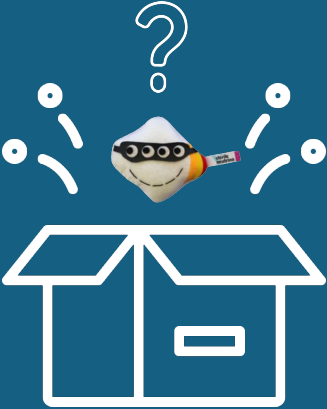
- Single detector  $\nu_\mu$  disappearance within the 3+1 sterile neutrino model
- Systematics treatment via covariance matrices and nuisance parameters
- Combined Neyman-Pearson for test statistic
- Feldman-Cousins corrections to sensitivity and data contours
- Staged unblinding procedure



# Fitting and statistical analysis

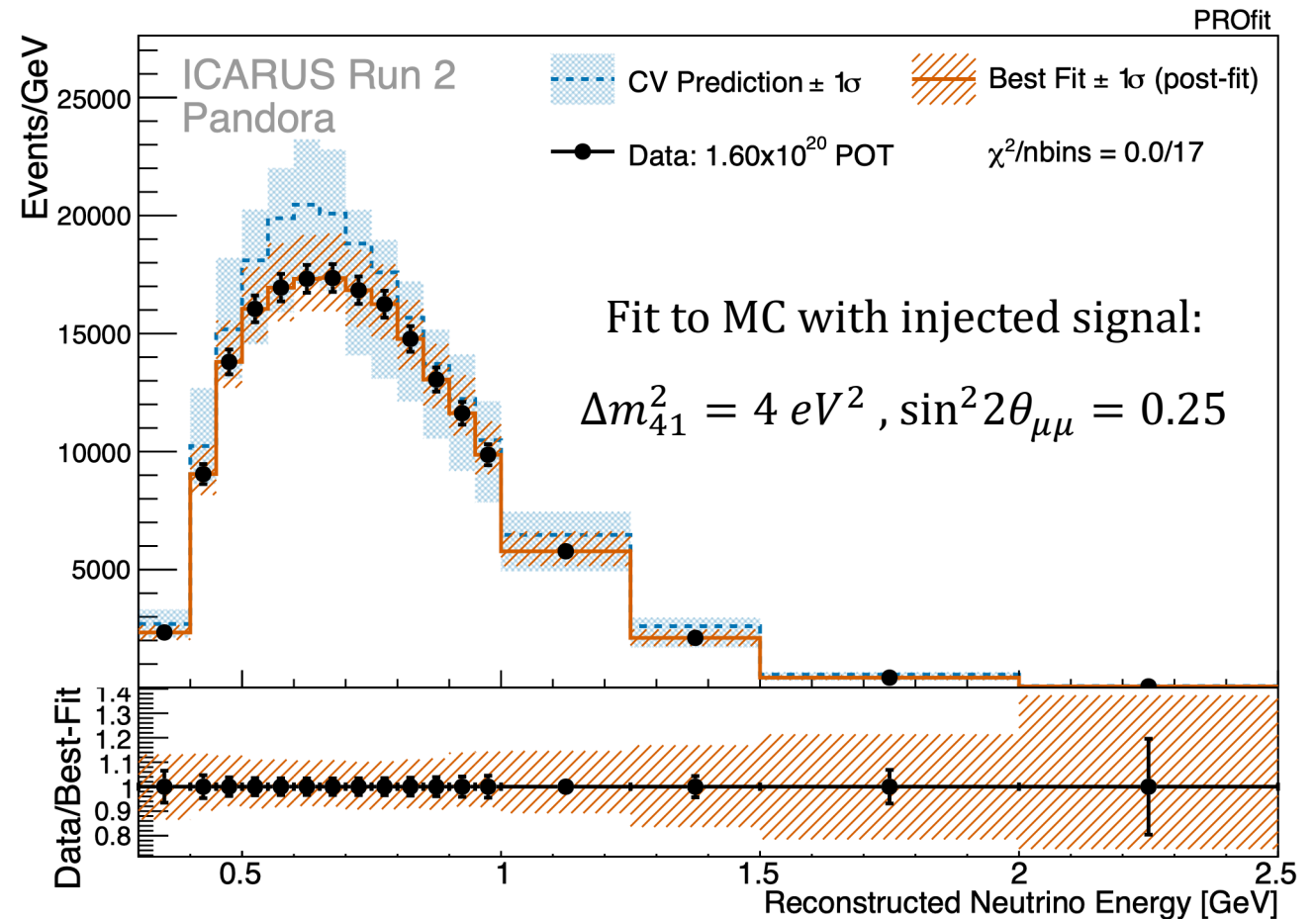
- Brand new statistical analysis framework developed for SBN: PROfit

- Main features used in this analysis:



Fit successfully recovers  
the injected signal.  
Ready to fit the data!

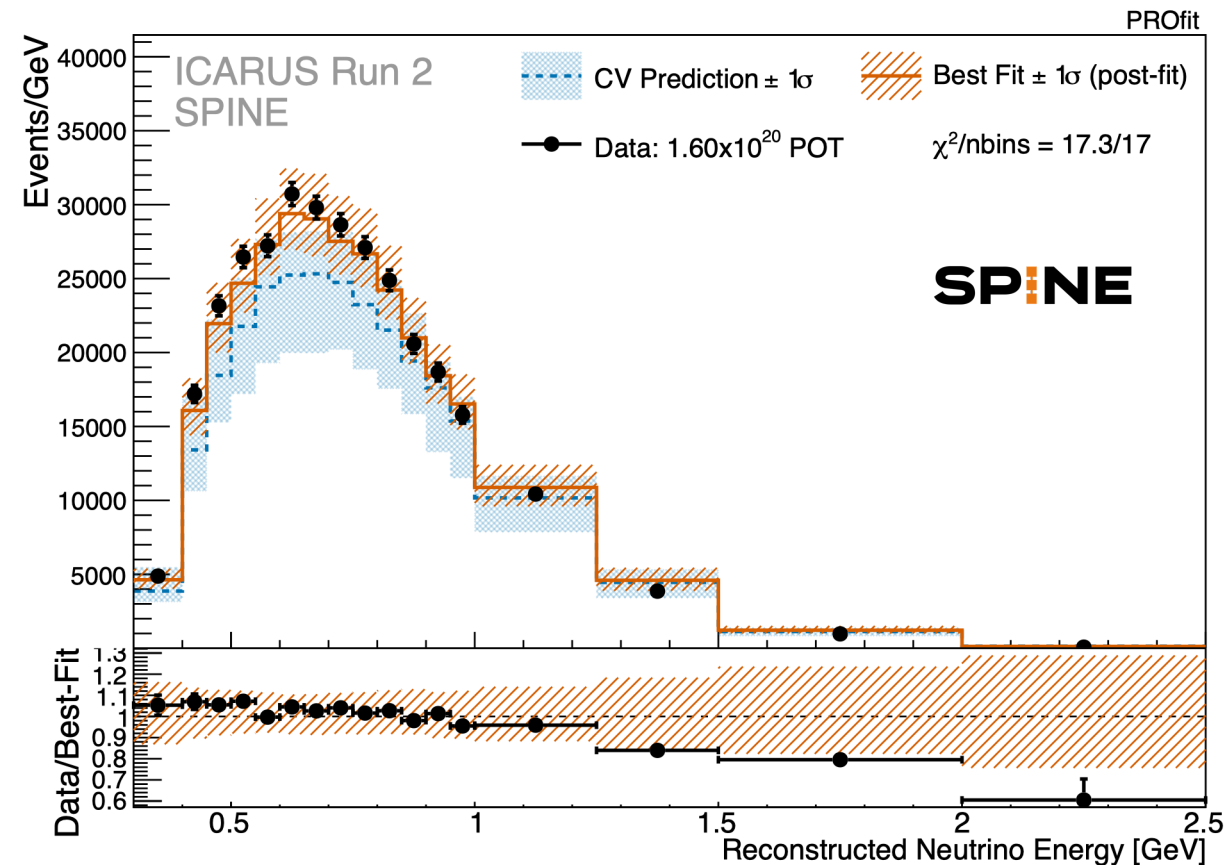
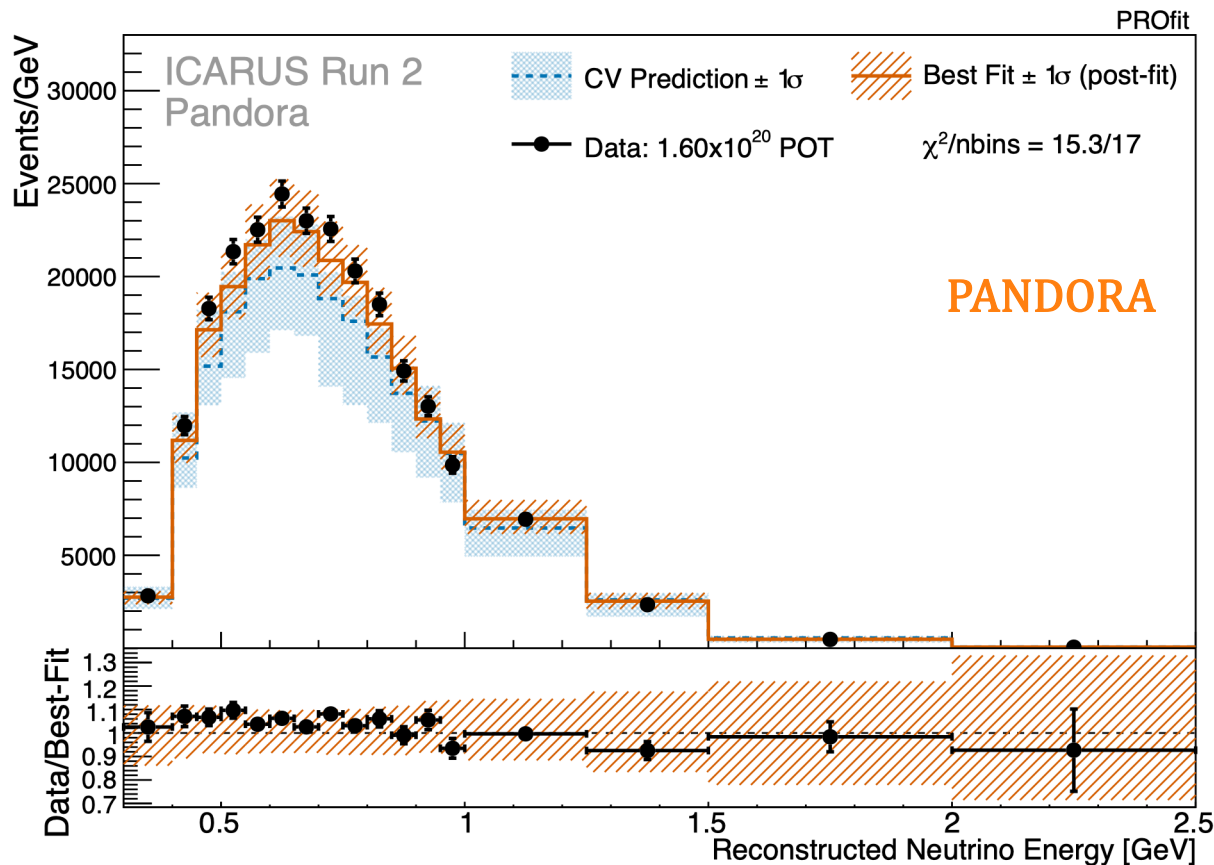
- Feldman-Cousins corrections to sensitivity and data contours
- Staged unblinding procedure



# Results: post-fit spectra

- Difference in  $\chi^2$  between fits with oscillations and only with nuisance parameters (null hypothesis) quantifies the significance for the 3+1 oscillation model

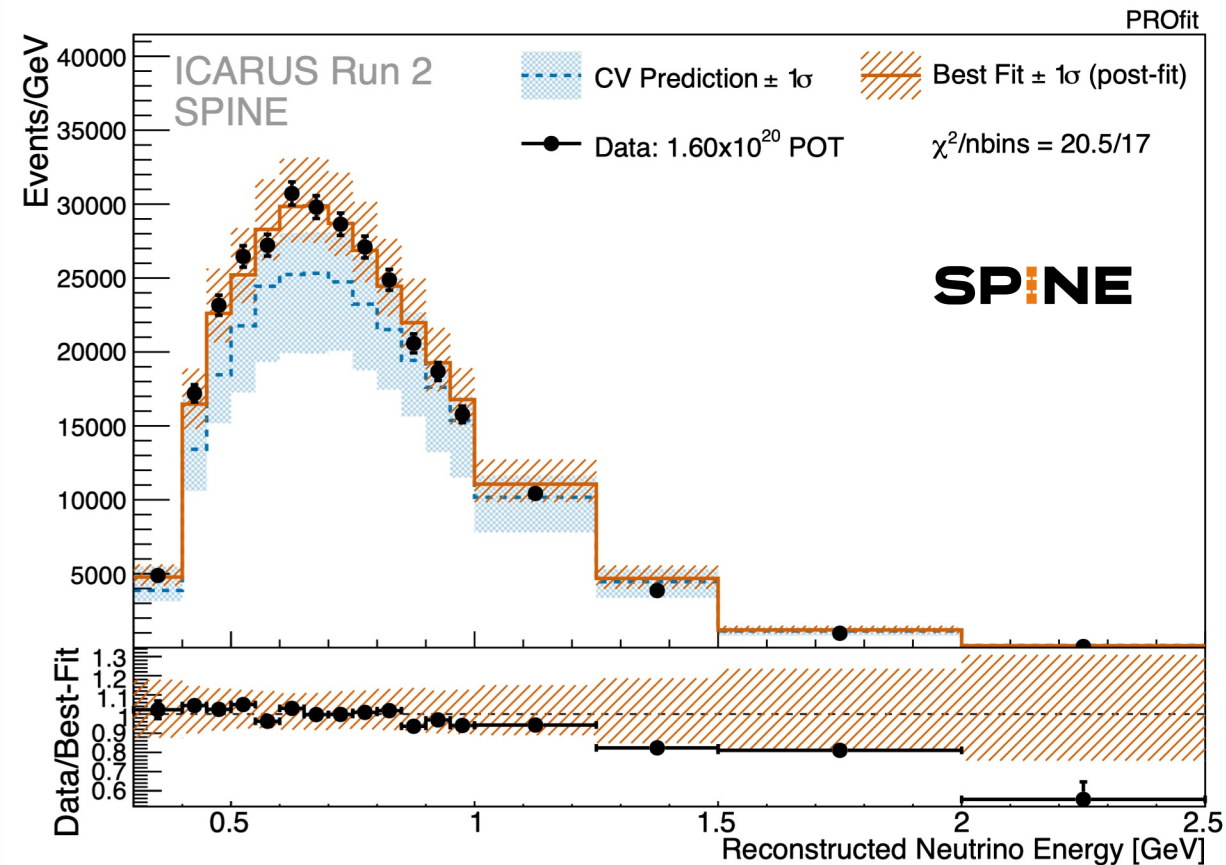
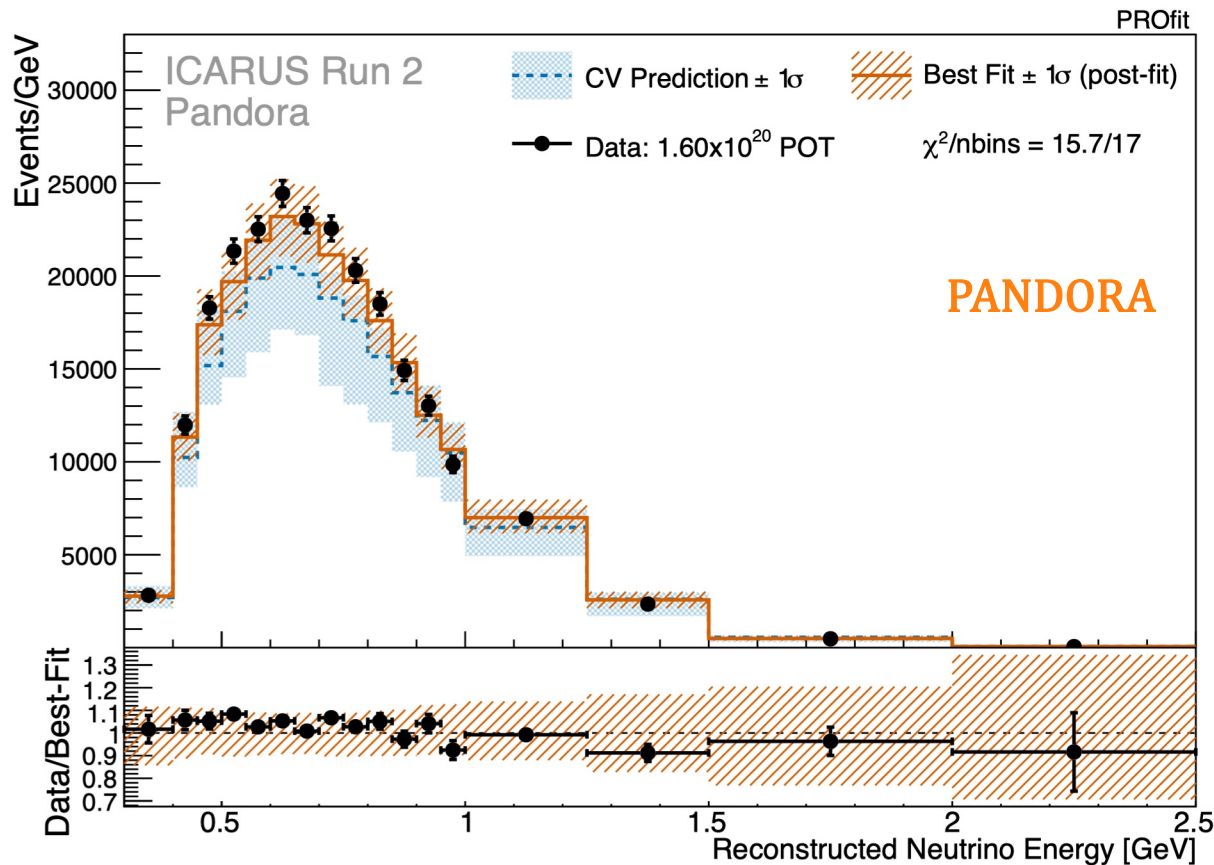
## Fit with oscillation parameters



# Results: post-fit spectra

- Difference in  $\chi^2$  between fits with oscillations and only with nuisance parameters (null hypothesis) quantifies the significance for the 3+1 oscillation model

## Fit to null hypothesis



# Fit results

- No evidence for  $\nu_\mu$  disappearance observed in the context of 3+1 sterile neutrino model
- Both fits consistent with no oscillation (after Feldman-Cousins correction)



Hence exclusion contours are reported

	Best fit $\sin^2 2\theta_{\mu\mu}$	Best fit $\Delta m_{41}^2$	$\chi^2$ null	$\chi^2$ osc	$\Delta\chi^2$	FC p-value
Pandora	0.07	10.2	15.7	15.3	0.4	0.91
SPINE	0.24	13.5	20.5	17.3	3.2	0.42

- Slightly higher significance for oscillation in SPINE fit result from highest energy bins



SPINE is more efficient than Pandora



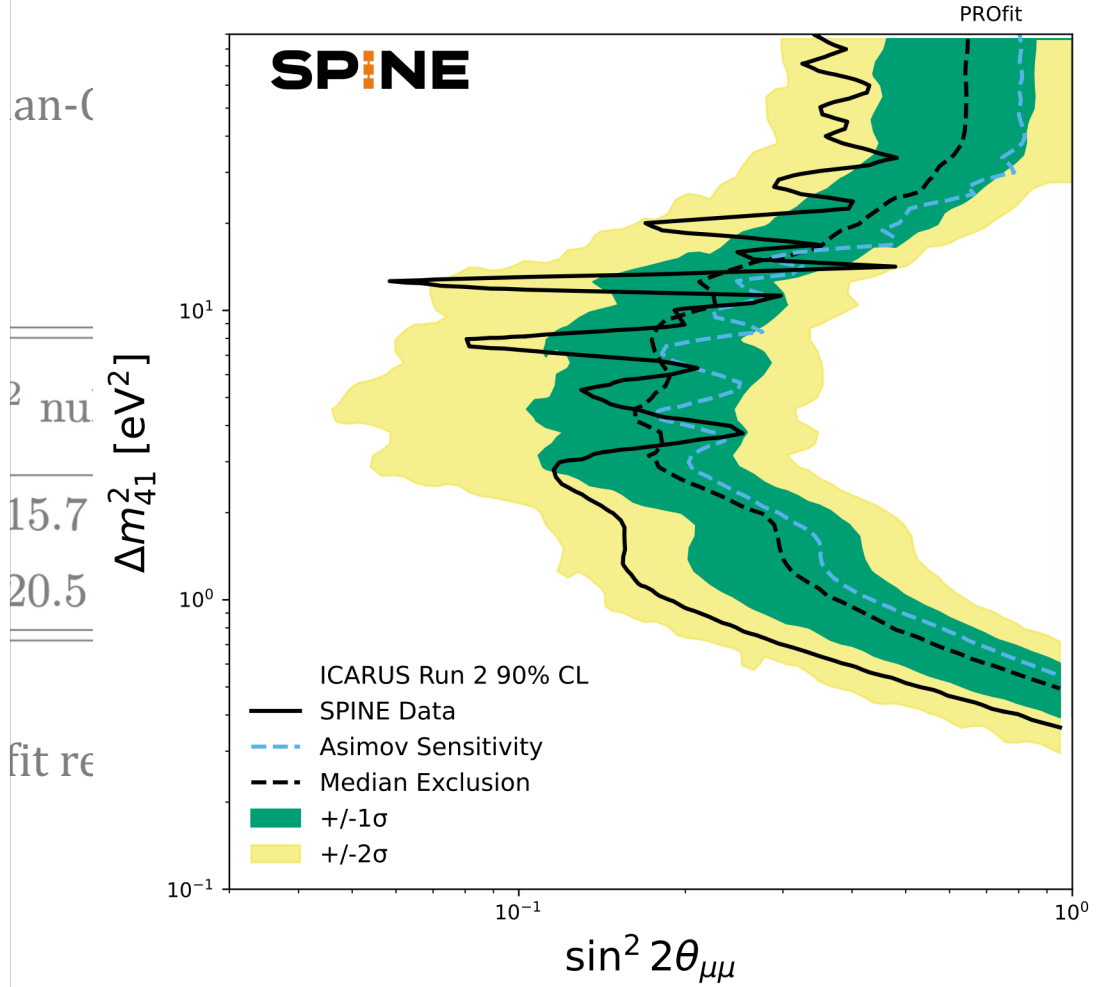
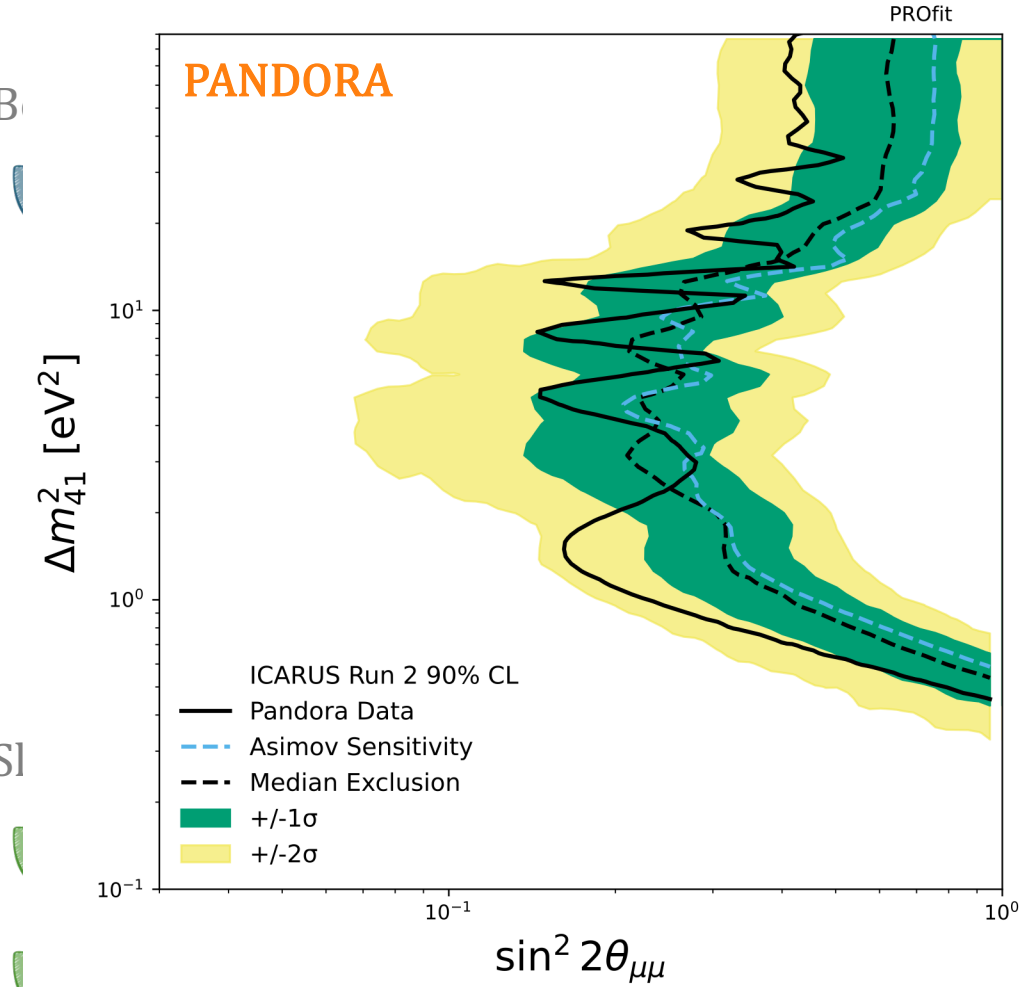
Less affected by systematic uncertainties

# Fit results

- No evidence for  $\nu_\mu$  disappearance observed in the context of 3+1 sterile neutrino model

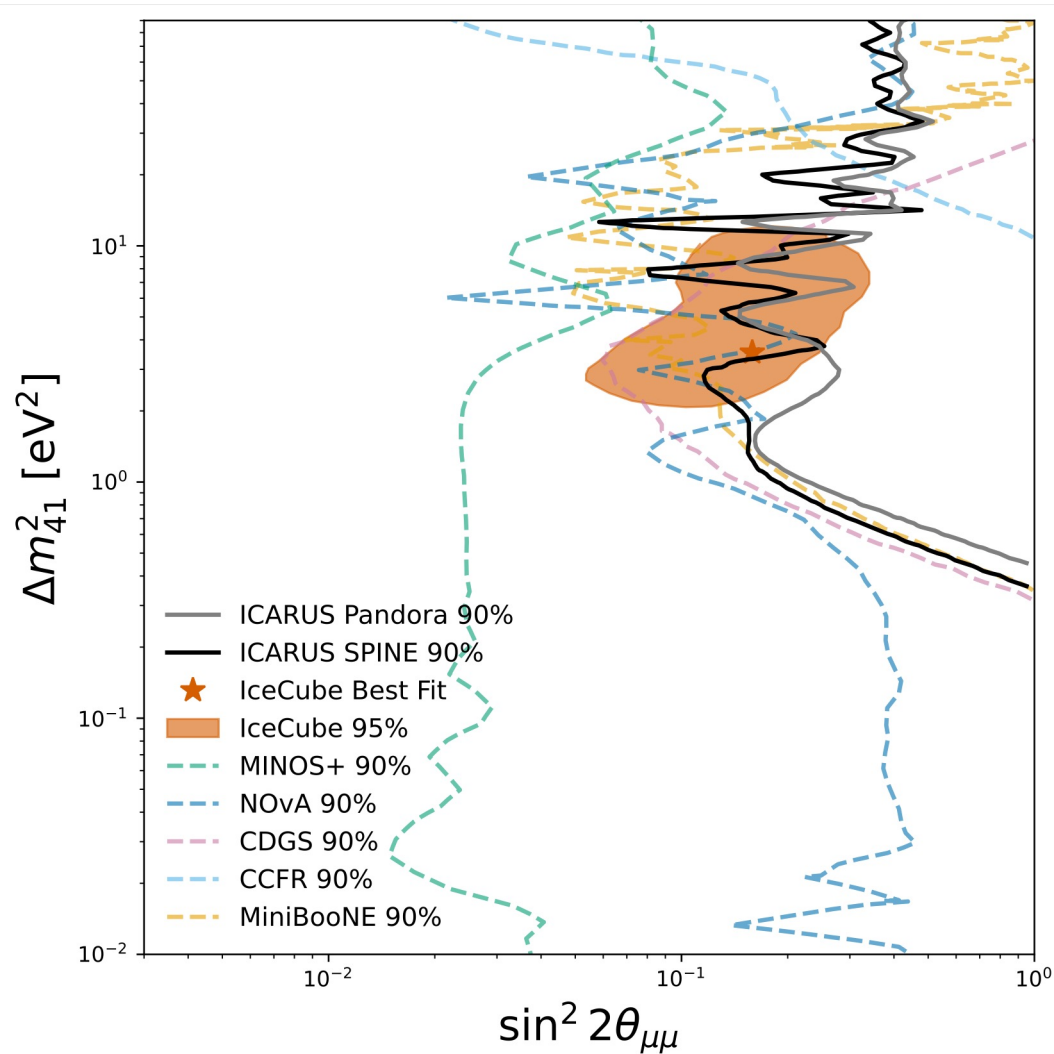
B

S



Less affected by systematic uncertainties

# Conclusions



- 90% Confidence level exclusion contours in context to actual world data
- Similar to other single-detector disappearance searches
- Systematics limited measurement
- Expect systematics to reduce from  $\sim 20\%$  to few percent with:
  - Improved detector modeling
  - Addition of  $\nu_e$  samples
  - near detector data



SBND jointly taking data from Run 4 ( $\sim$  Jan 2025)

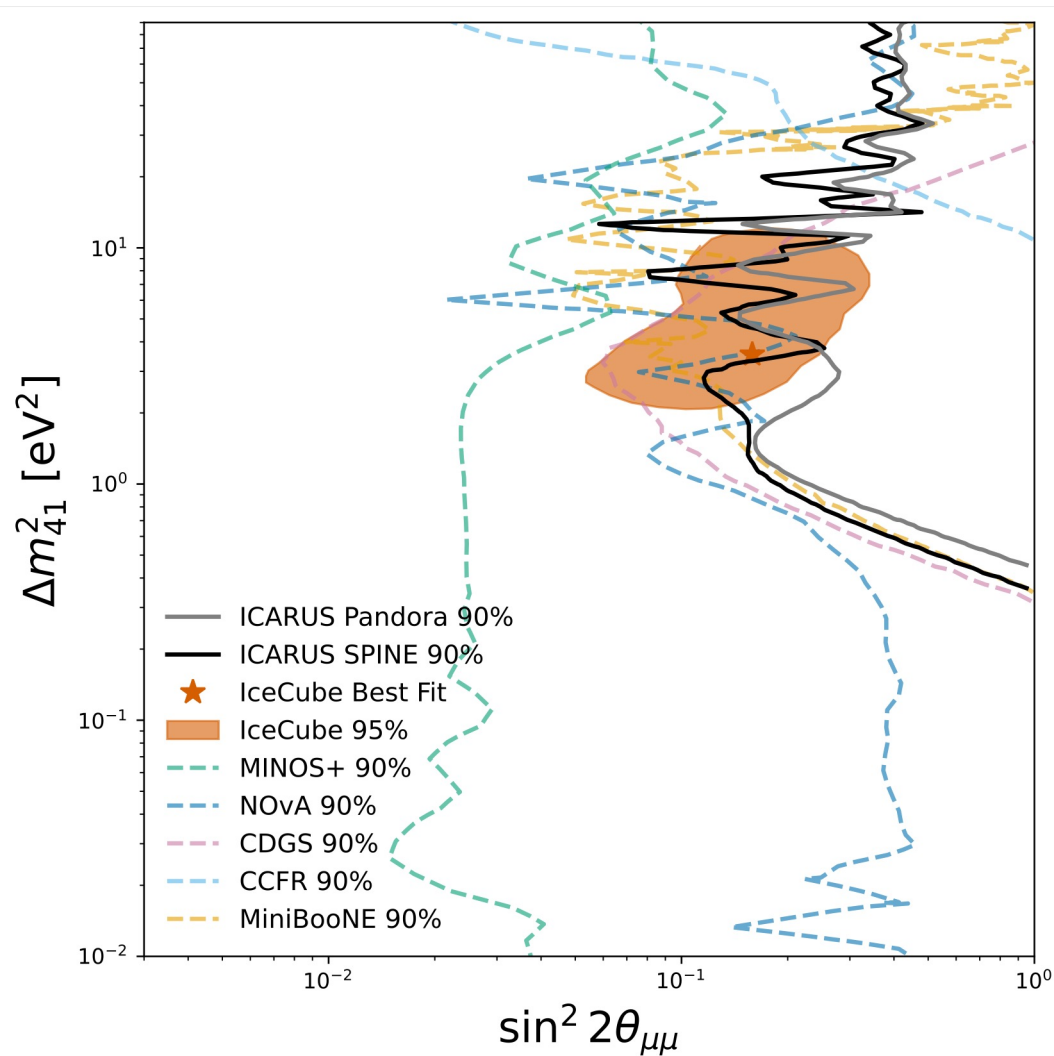
PRESS RELEASE

**First neutrinos detected at Fermilab short-baseline detector**

September 10, 2024

More details [here](#)

# Conclusions



- 90% Confidence level exclusion contours in context to actual world data
- Similar to other single-detector disappearance searches
- Systematics limited measurement
- Expect systematics to reduce from  $\sim 20\%$  to few percent with:
  - Improved detector modeling
  - Addition of  $\nu_e$  samples
  - near detector data
- **Proved ICARUS' capability and readiness of analysis tools**
- **Currently working to combine near (SBND) and far (ICARUS) detectors data**



See here [\[1\]](#) and [\[2\]](#) for more details!

Backup slides

# Neutrino mixing and oscillations

- Neutrinos beyond the Standard Model

$$|\nu_\alpha\rangle = \sum_{k=1,2,3} U_{\alpha k}^* |\nu_k(0)\rangle \quad \xrightarrow{|\nu_k(t)\rangle = e^{-iE_k t} |\nu_k(0)\rangle} \quad \langle\nu_\beta| = \sum_{j=1,2,3} \langle\nu_j(0)| U_{\beta j}$$

Production:  $\nu_e, \nu_\mu, \nu_\tau$       Propagation:  $\nu_1, \nu_2, \nu_3$       Detection:  $\nu_e, \nu_\mu, \nu_\tau$   
 flavor eigenstates      mass eigenstates      flavor eigenstates

- Pontecorvo-Maki-Nakagawa-Sakata (PMNS) matrix

$$\begin{pmatrix} \nu_e \\ \nu_\mu \\ \nu_\tau \end{pmatrix} = \begin{pmatrix} 1 & 0 & 0 \\ 0 & c_{23} & s_{23} \\ 0 & -s_{23} & c_{23} \end{pmatrix} \begin{pmatrix} c_{13} & 0 & s_{13}e^{-i\delta} \\ 0 & 1 & 0 \\ -s_{13}e^{i\delta} & 0 & c_{13} \end{pmatrix} \begin{pmatrix} c_{12} & s_{12} & 0 \\ -s_{12} & c_{12} & 0 \\ 0 & 0 & 1 \end{pmatrix} \begin{pmatrix} e^{i\alpha_1} & 0 & 0 \\ 0 & e^{i\alpha_2} & 0 \\ 0 & 0 & 1 \end{pmatrix} \begin{pmatrix} \nu_1 \\ \nu_2 \\ \nu_3 \end{pmatrix}$$

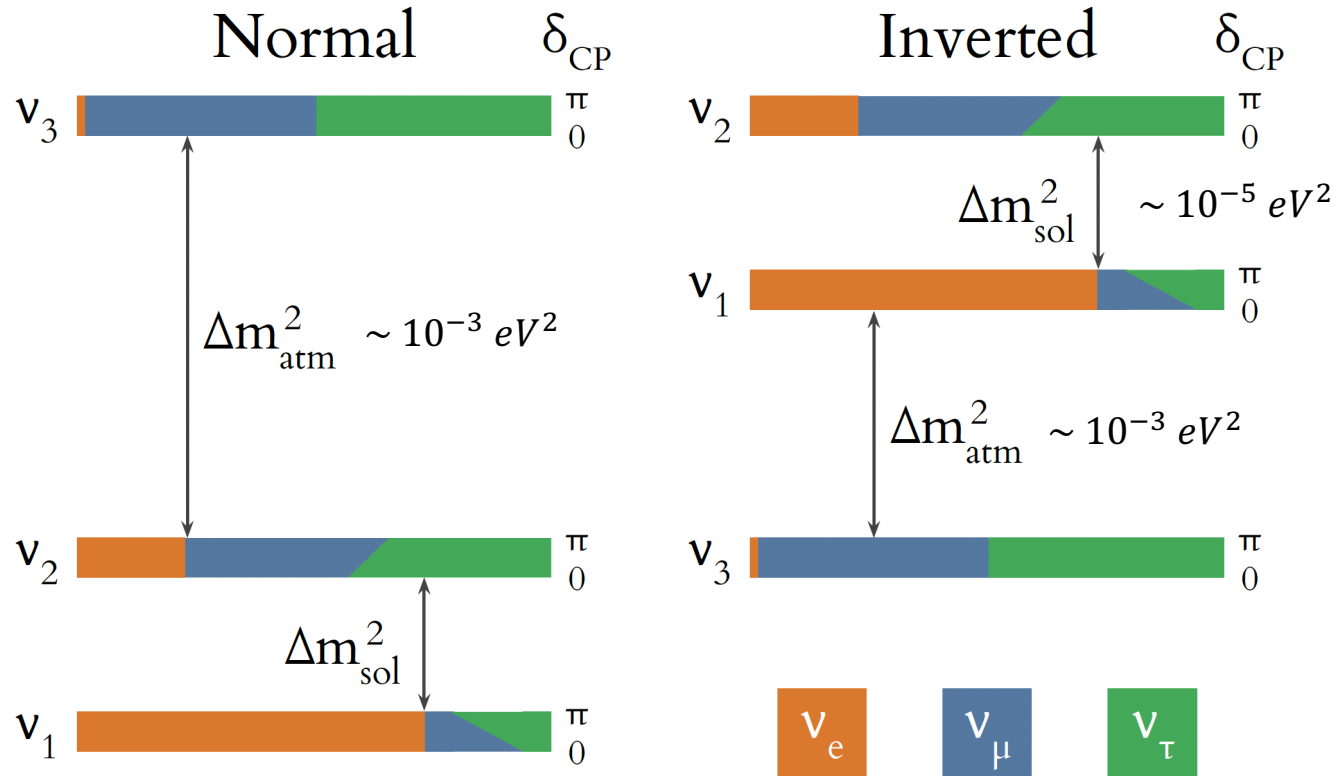
Atm. + accelerator      Reactors      Reactor + solar      Majorana  
 $\nu_\mu \rightarrow \nu_\tau$        $\nu_\mu \rightarrow \nu_e$        $\nu_e \rightarrow \nu_{\mu,\tau}$

$$c_{ij} = \cos \theta_{ij} \\ s_{ij} = \sin \theta_{ij}$$

# Neutrino mixing and oscillations

- Oscillation probability

$$P(\nu_\alpha \rightarrow \nu_\beta) = \delta_{\alpha\beta} - 4 \sum_{k>j} \Re[U_{\alpha k}^* U_{\beta k} U_{\alpha j} U_{\beta j}^*] \sin^2 \left( \frac{\Delta m_{kj}^2 L}{4E} \right) \pm 2 \sum_{k>j} \Im[U_{\alpha k}^* U_{\beta k} U_{\alpha j} U_{\beta j}^*] \sin \left( \frac{\Delta m_{kj}^2 L}{2E} \right)$$



# Beyond $3\nu$

- 3+1 the simplest model: addition of a new sterile massive state
  - Massive  $\rightarrow$  to explain the observed data  $m_4 \gg m_i$ , therefore  $\Delta m_{4i}^2 \sim eV^2 \quad \forall i \in [1,2,3]$
  - Sterile  $\rightarrow$  to avoid clashing with the number of active neutrinos measured by the LEP experiment,  $|U_{\alpha 4}| \ll 1$  for  $\alpha \in [e, \mu, \tau]$
- In order to study this fourth mass state, one needs a  $L/E \sim \mathcal{O}(1 \text{ km/GeV})$ , much shorter than the one needed to study the atmospheric and solar oscillations  Small sensitivity to  $\Delta m_{sol}^2$  and  $\Delta m_{atm}^2$ 
  - **Short baseline approximation**  $\Delta m_{sol}^2 \approx \Delta m_{atm}^2 \approx 0$

$$\begin{pmatrix} \nu_e \\ \nu_\mu \\ \nu_\tau \\ \nu_s \end{pmatrix} = \begin{pmatrix} U_{e1} & U_{e2} & U_{e3} & U_{e4} \\ U_{\mu 1} & U_{\mu 2} & U_{\mu 3} & U_{\mu 4} \\ U_{\tau 1} & U_{\tau 2} & U_{\tau 3} & U_{\tau 4} \\ U_{s1} & U_{s2} & U_{s3} & U_{s4} \end{pmatrix} \begin{pmatrix} \nu_1 \\ \nu_2 \\ \nu_3 \\ \nu_4 \end{pmatrix}$$

Appearance probability

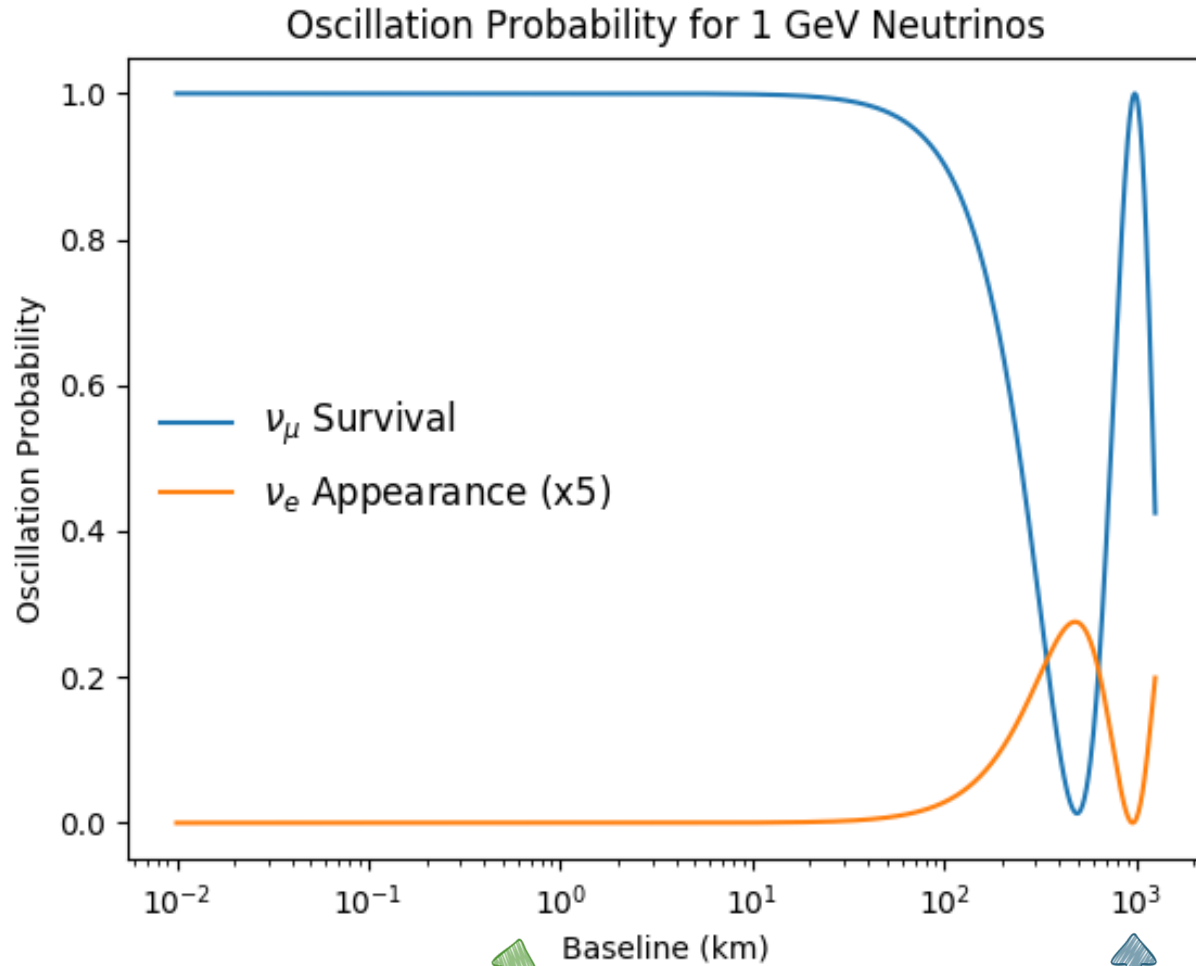
$$P^{SBL}(\nu_\alpha \rightarrow \nu_\beta) \simeq \sin^2 2\theta_{\alpha\beta} \sin^2 \left( 1.27 \Delta m_{41}^2 \frac{L}{E} \right)$$

Disappearance probability

$$P^{SBL}(\nu_\alpha \rightarrow \nu_\alpha) \simeq 1 - \sin^2 2\theta_{\alpha\alpha} \sin^2 \left( 1.27 \Delta m_{41}^2 \frac{L}{E} \right)$$

\* where  $\sin^2 2\theta_{\alpha\beta} = 4|U_{\alpha 4}|^2|U_{\beta 4}|^2$  and  $\sin^2 2\theta_{\alpha\alpha} = 4(1 - |U_{\alpha 4}|^2)|U_{\alpha 4}|^2$

# Short Baseline Neutrino oscillations



Short baseline  
experiments



Long baseline experiments

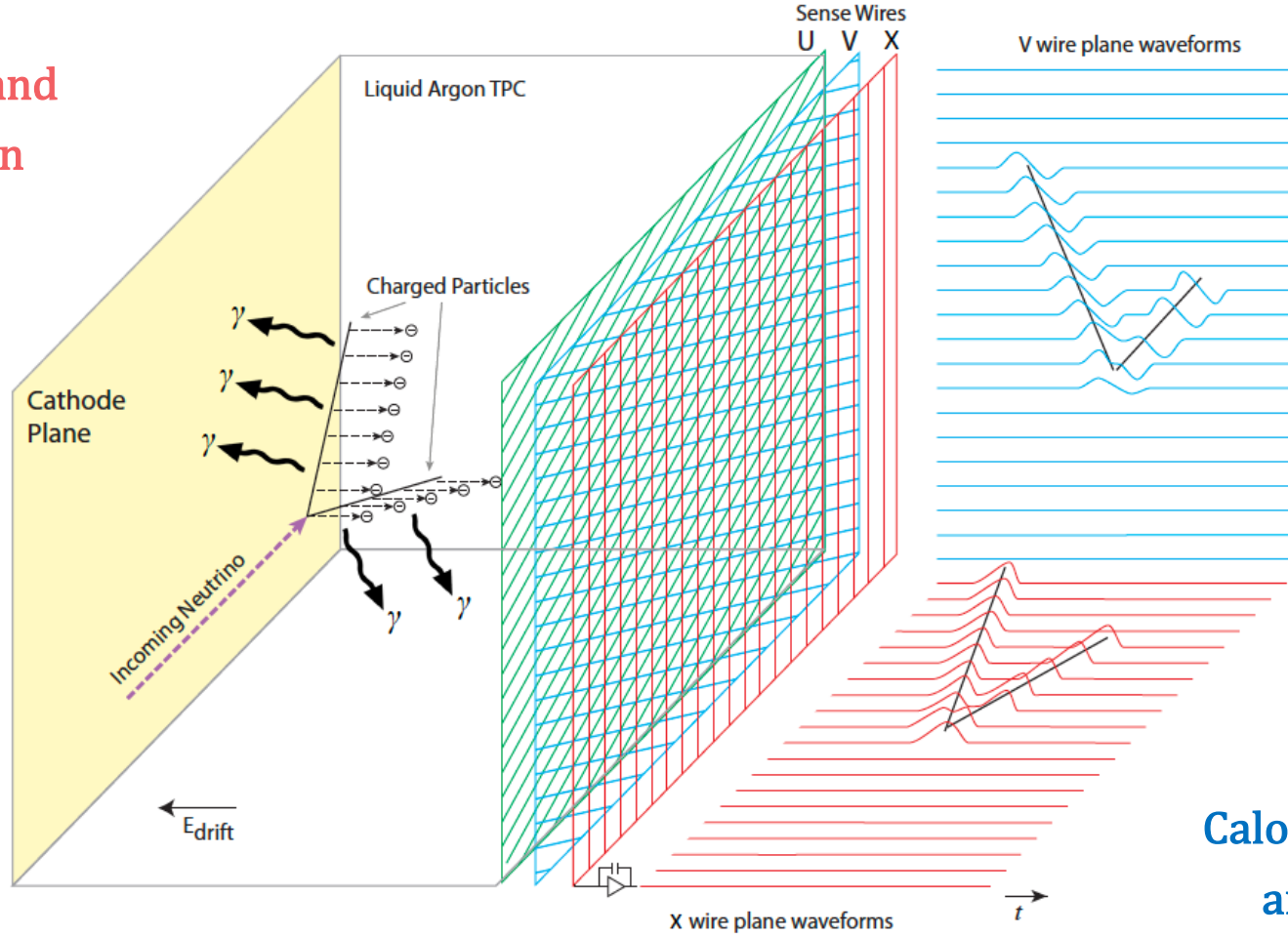
- We observe significant oscillations at large values of  $L/E$  but – based on the already measured mass splittings – we do not expect to see neutrino oscillation at small values of  $L/E$
- Any  $\nu_\mu$  disappearance or  $\nu_e$  appearance at these  $L/E$  values would require a larger mass splitting, which would require at least 1 additional neutrino mass state → new physics!

# LArTPC technology

Excellent 3D imaging and mm spatial resolution

MeV energy threshold

Prompt scintillation light for timing



Good electron-photon discrimination

Scalable detector to mass and drift length

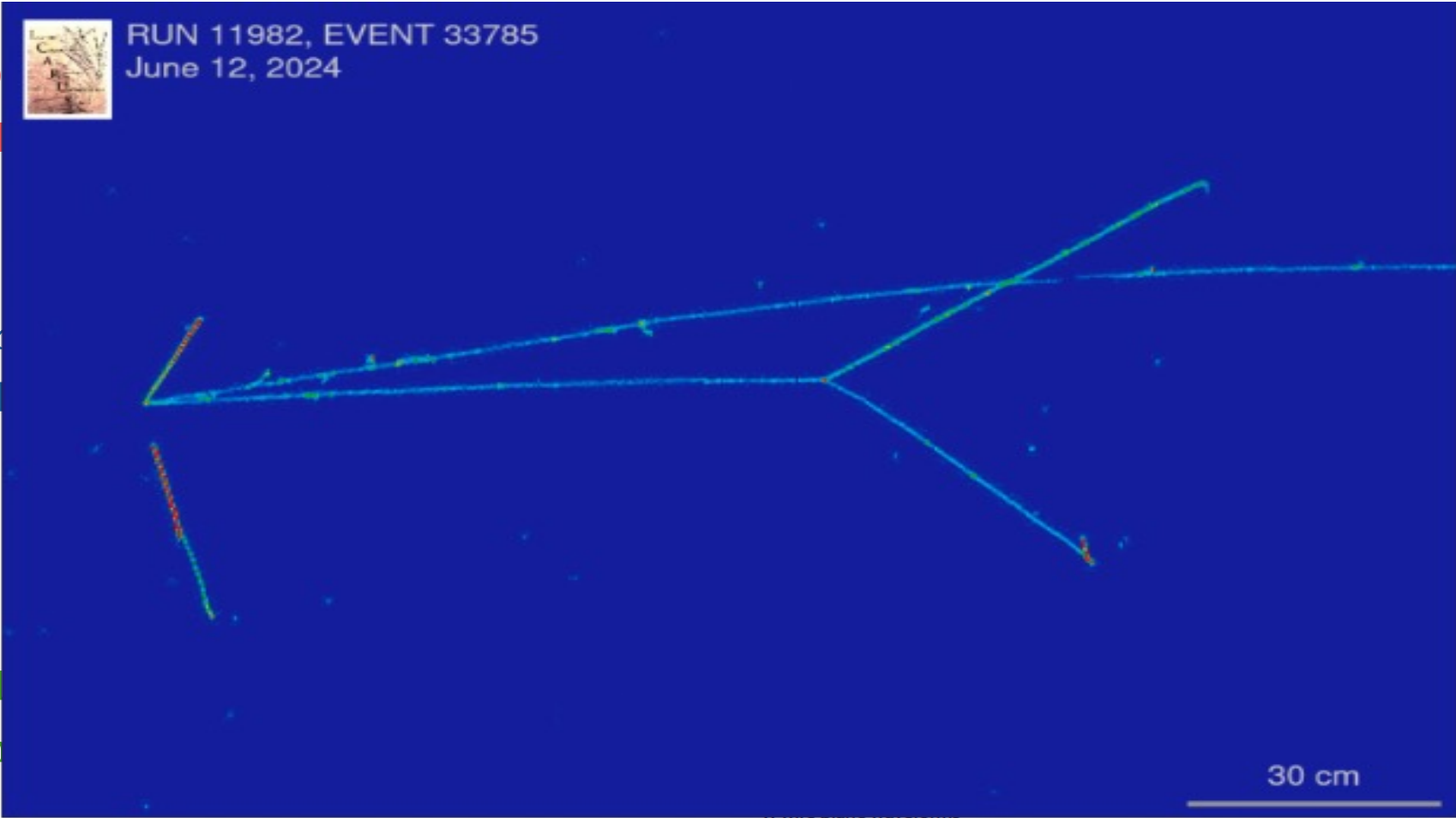
Calorimetry and tracking for PID and energy reconstruction

# LArTPC technology

Excellent 3D  
mm spatial

MeV ener  
threshol

Prompt scintil  
light for tim



Good electron-photon  
discrimination

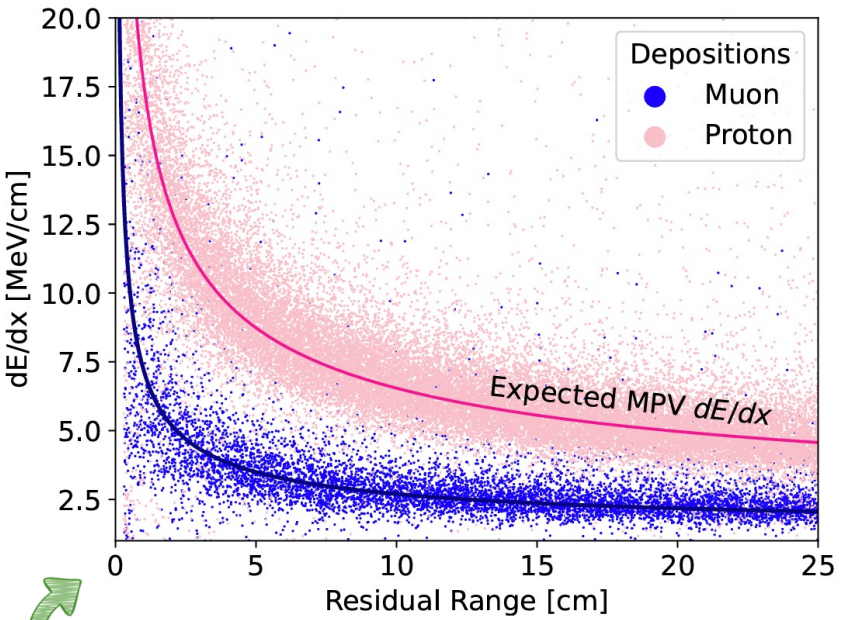
scalable detector to  
mass and drift length

and tracking for PID  
reconstruction

# ICARUS at FNAL most recent results

- Calibration and simulation of ionization signal and electronics noise

[P. Abratenko et al 2025 JINST 20 P01032](#)



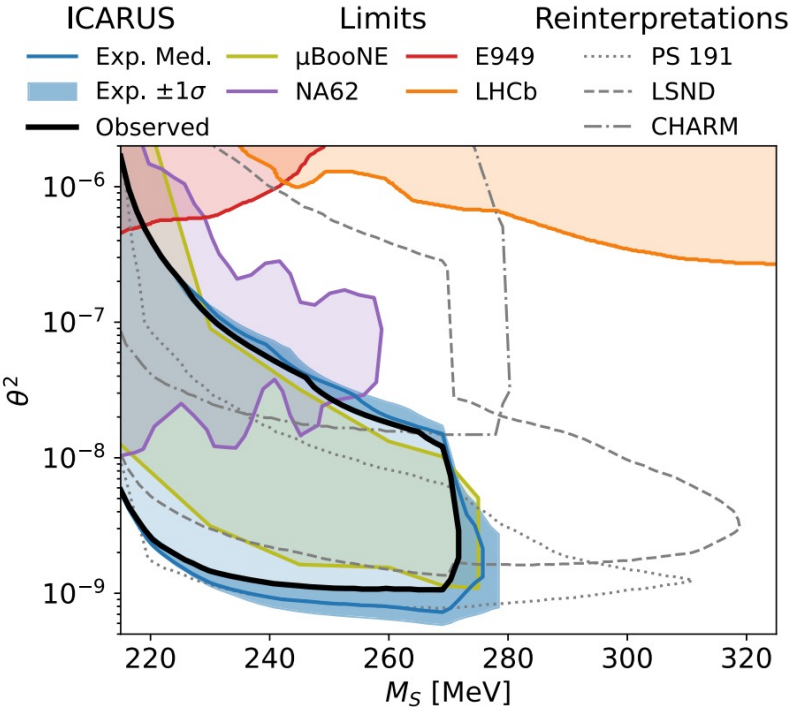
- Angular dependent measurement of electron-ion recombination in LAr

[P. Abratenko et al 2025 JINST 20 P01033](#)

- Search for long-lived particle decay to two muons

[Phys. Rev. Lett. 134, 151801](#)

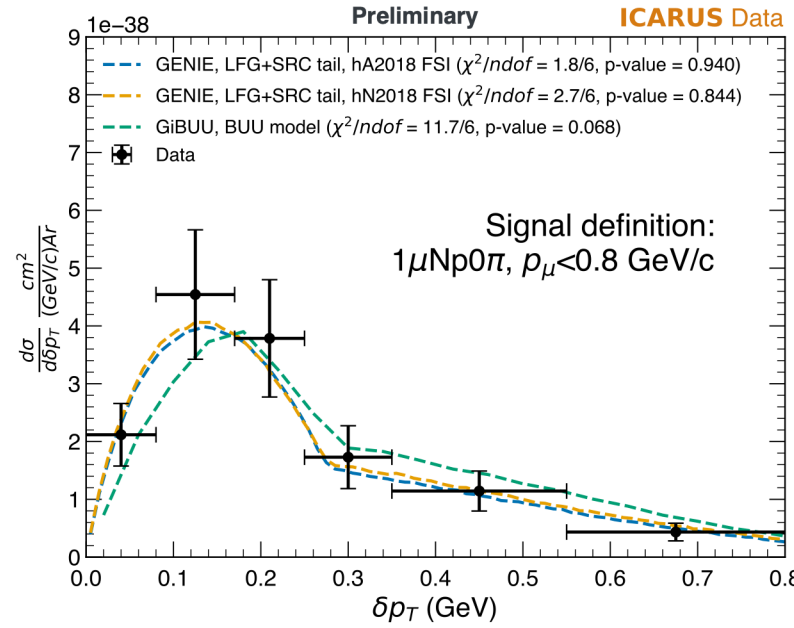
## Higgs Portal Scalar Exclusion



- Operation of the trigger system

[F. Abd Alrahman et al 2025 JINST 20 P10044](#)

- Muon neutrino cross-section measurement using the NuMI beam off axis



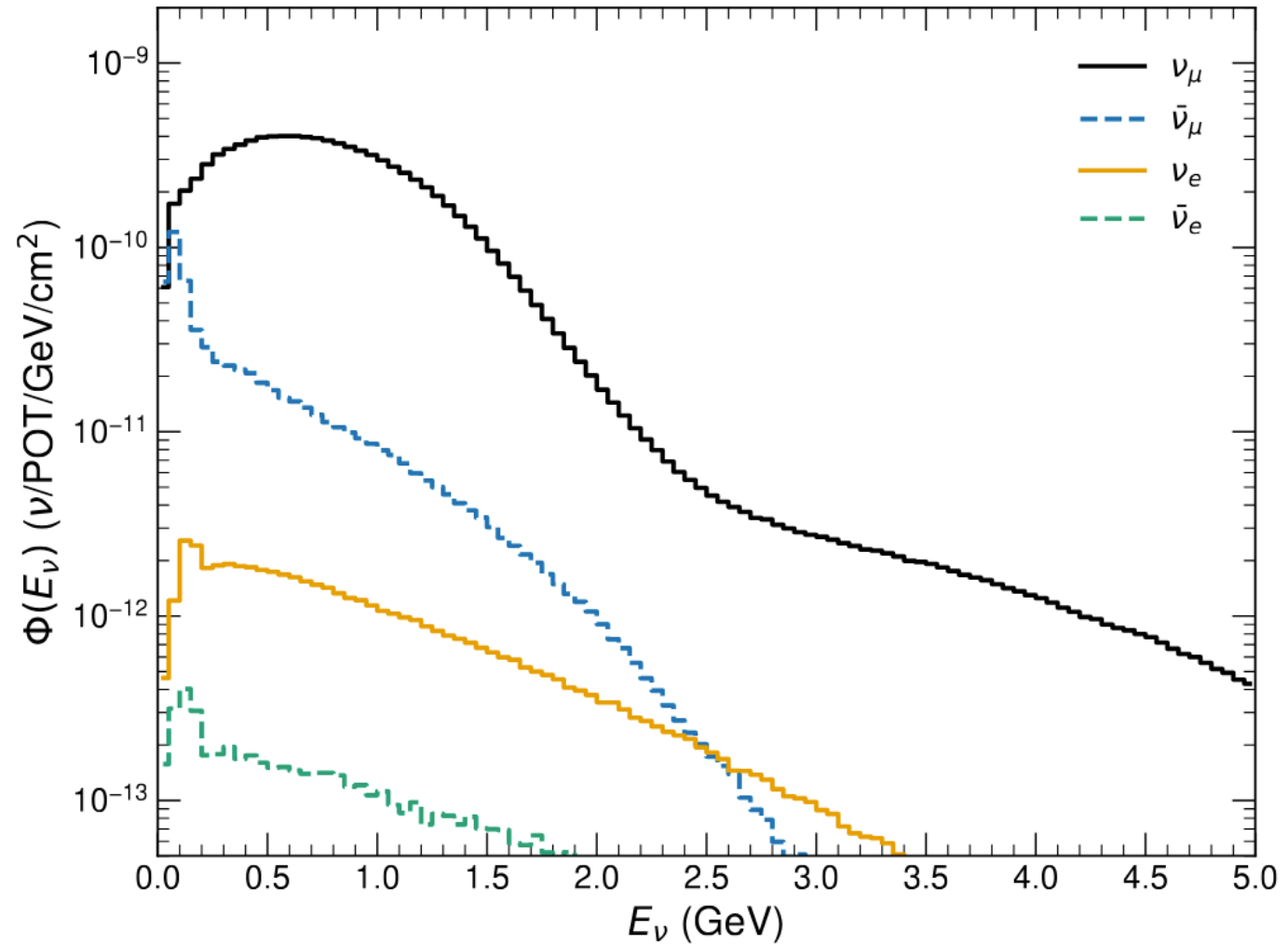
- See more details in the October 2025 Fermilab colloquium [here](#)

# BNB Flux prediction

Total predicted BNB flux by neutrino species at ICARUS.

The flux simulation was developed by MiniBooNE and MicroBooNE and is based on Geant4, with corrections applied to the pion production cross section using a Sanford--Wang parameterization fitted to HARP and E910 data.

Parent hadron decays to neutrinos are sampled over the front face of the ICARUS detector, where the flux is predicted to vary by less than 4%.

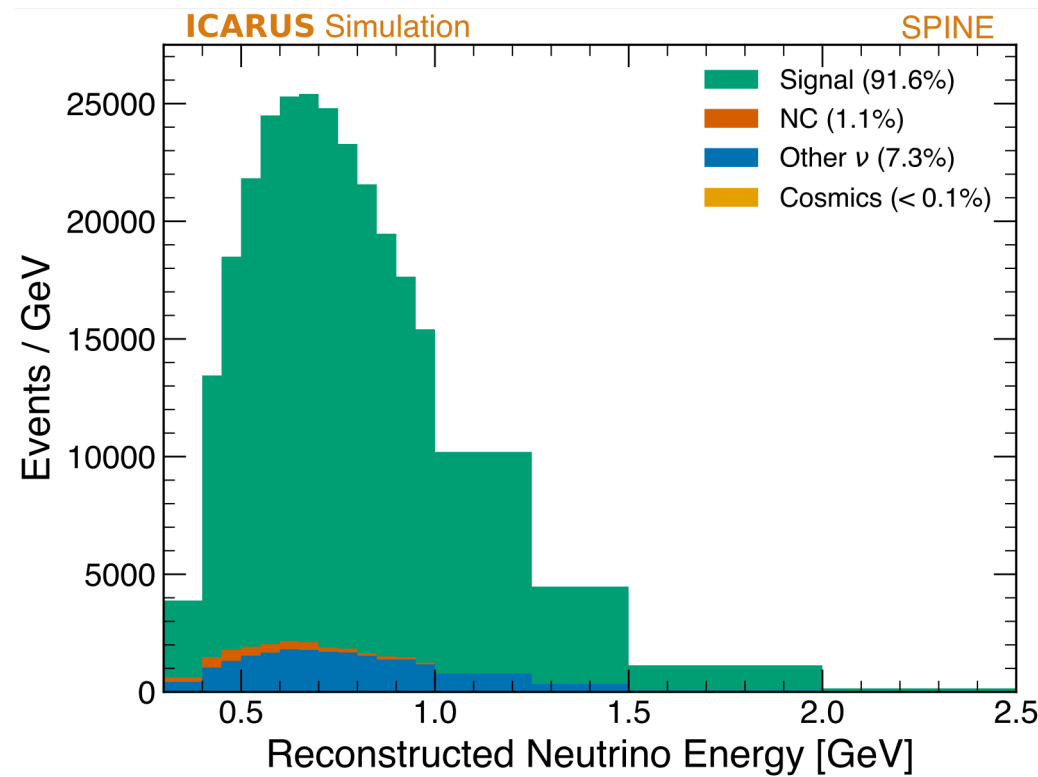
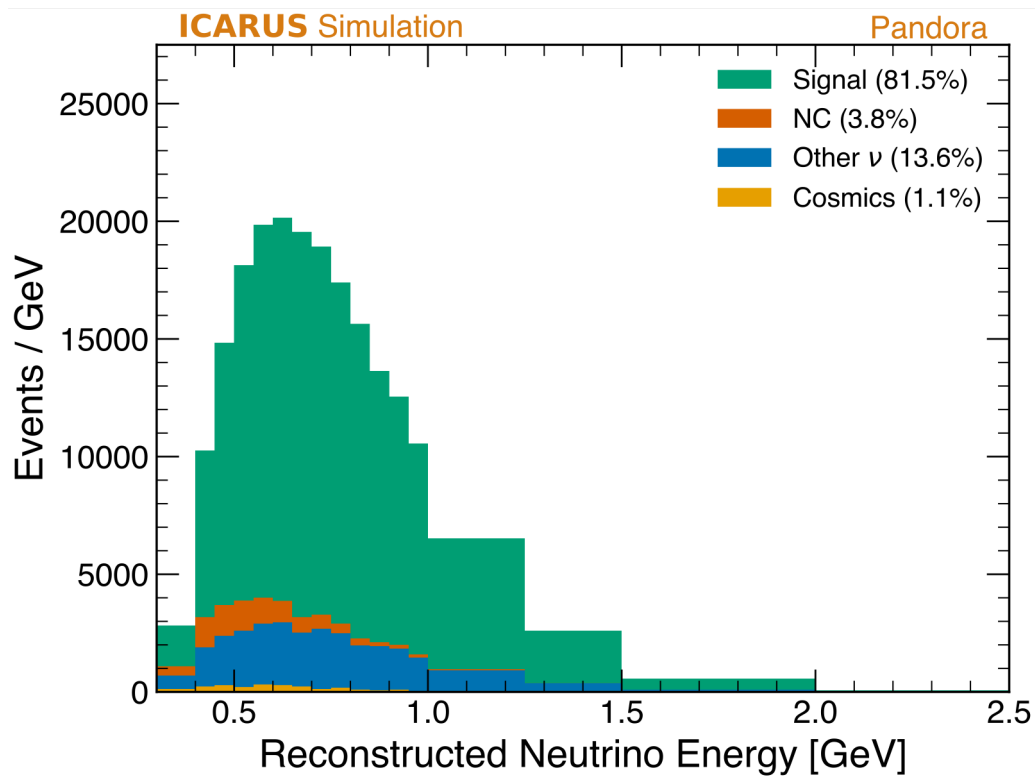




# Event selection

- Fully contained  $\nu_\mu$  CC within fiducial volume
- Only one  $\mu$  with  $L_\mu > 50$  cm ( $p_\mu > 226$  MeV/c)

- At least a proton with  $E_{dep} > 50$  MeV
- No additional  $\gamma$  or  $\pi^\pm$  with  $E_{dep} > 25$  MeV
- Cosmic rejection based on charge, light + CRT (Pandora) or beam timing (SPINE) information

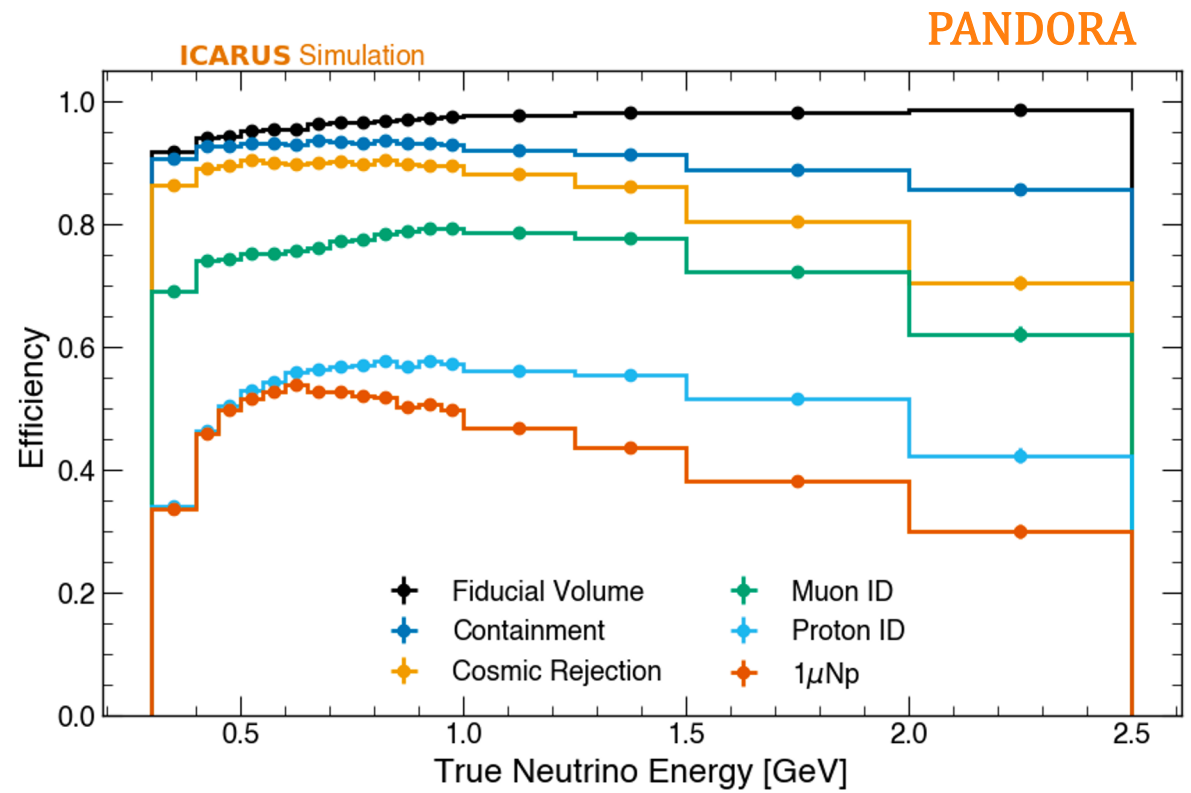


\*Event kinematic reconstruction from range-based measurements

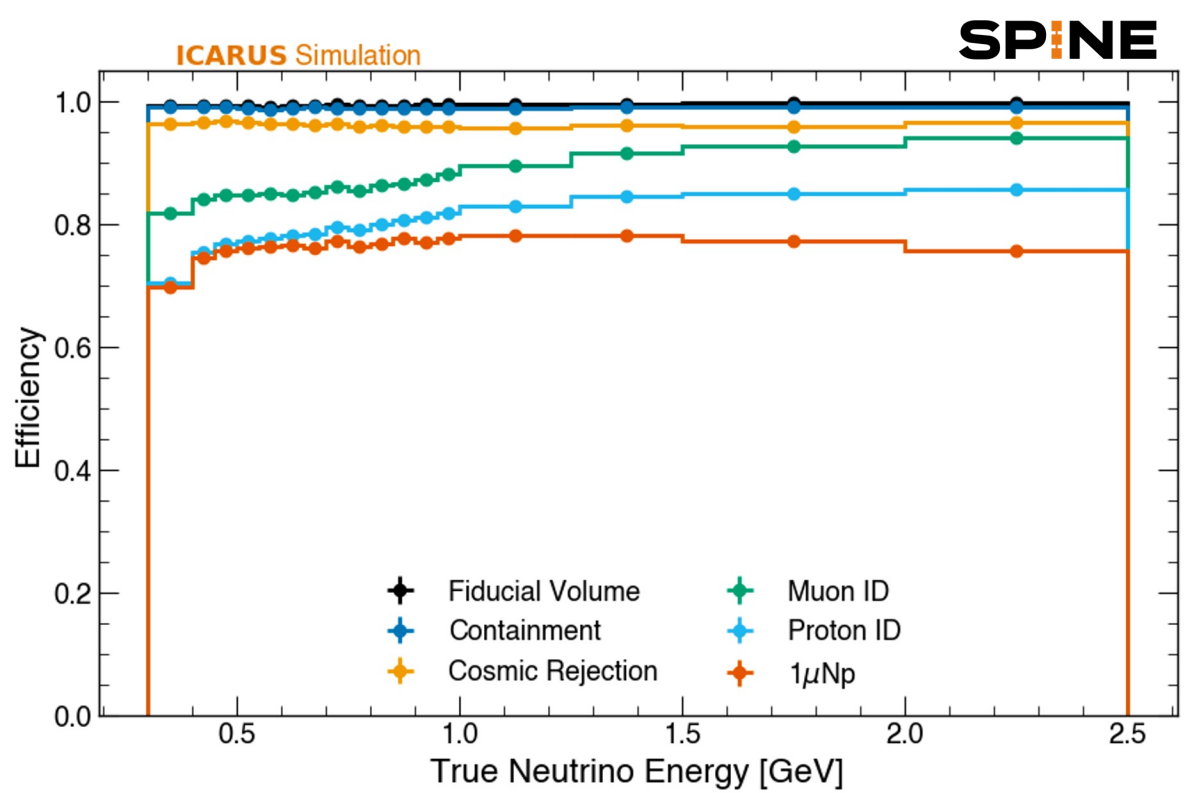


# Event selection

- Pandora: 48.5% global efficiency and 81.5% purity



- SPINE: 77% global efficiency and 91.6% purity



- Quoted numbers with respect to target sample (1μNp) and validated through visual scanning of the events

# Selection performance

- Efficiency and purity quoted with respect to the target sample. Many of the “background” events are true  $\nu_\mu$  CC

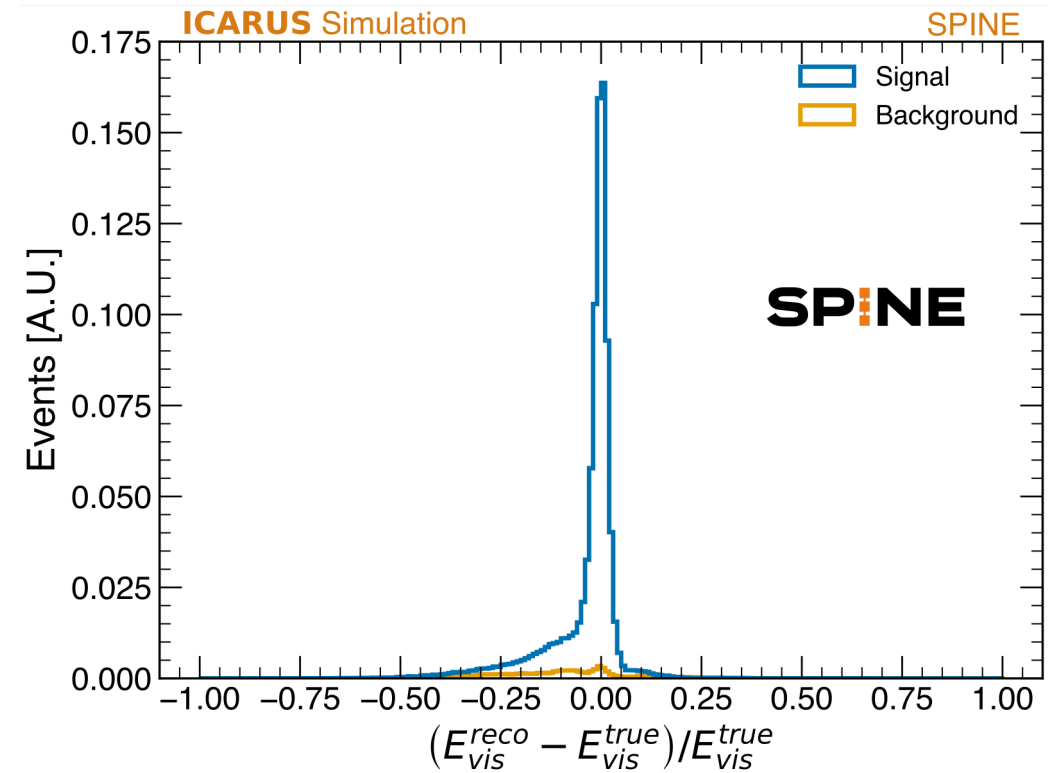
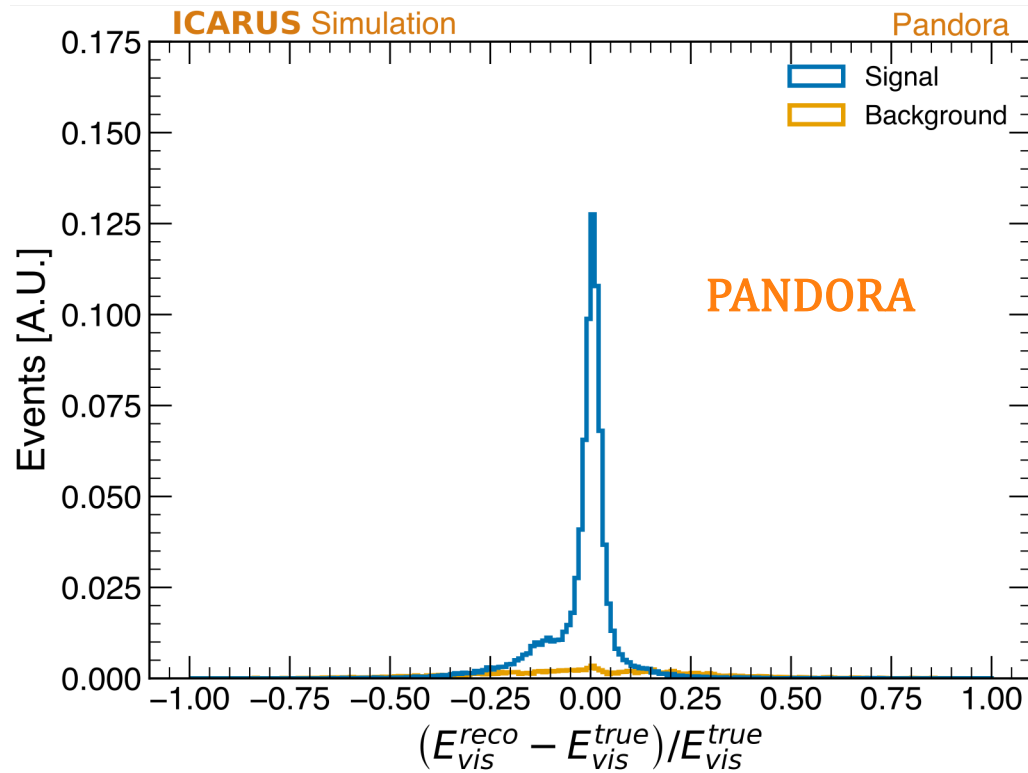
Selection Cut - Efficiency	Pandora [%]	SPINE [%]
No Cut	100	100
Reconstructed Vertex in FV	96.8	99.4
Containment	92.4	98.9
Cosmic Rejection	88.3	96.0
Muon ID	76.9	87.5
Proton ID	55.2	80.6
No Pions	50.7	78.2
No Showers	48.5	77.0

Selection Cut - Purity	Pandora [%]	SPINE [%]
No Cut	< 0.1	< 0.1
Reconstructed Vertex in FV	0.8	0.8
Containment	1.2	6.5
Cosmic Rejection	24.9	26.1
Muon ID	45.2	52.4
Proton ID	65.1	68.1
No Pions	71.4	80.1
No Showers	81.5	91.6

# Reconstruction performance

$$E_\nu = E_\mu + \sum KE_p + BE_p$$

- Good energy reconstruction for signal events
  - ↳ low-side tail coming from track-length mis-reconstruction
- Background is poorly reconstructed due to incorrect particle ID

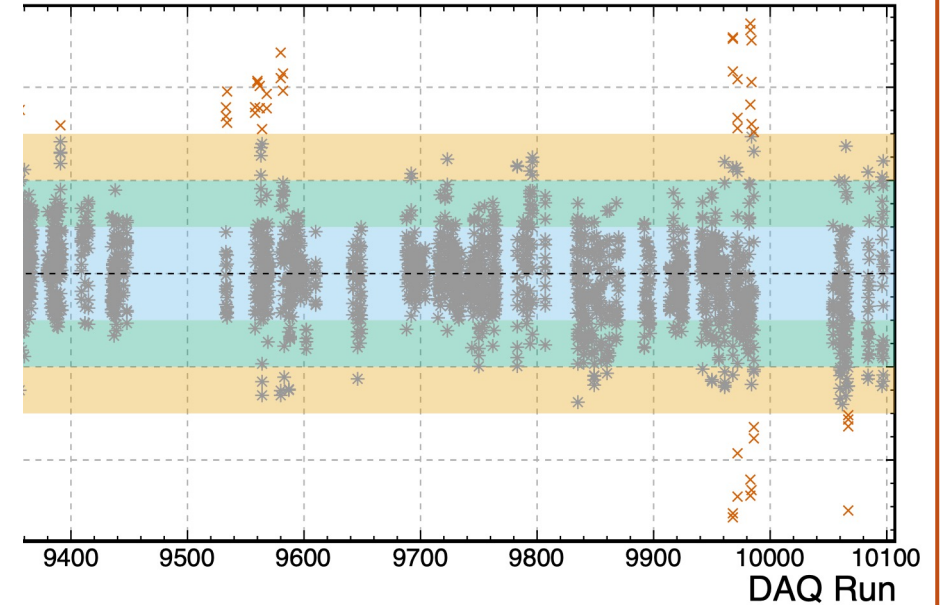


\*Event kinematic reconstruction from range-based measurements

# Data and Beam quality

- Today's result is based on BNB data collected in ICARUS Run 2 (2022-2023)
- Data quality is assessed using:
  - Detector operation: nominal operating conditions
  - Low-level metrics for a given run within  $3\sigma$  of global mean: number of hits per track, average photoelectrons per flash, ...
- Beam quality is assessed using BNB beamline monitors
  - Non-zero beam intensity
  - Nominal horn current
  - Centering of beam on target
- Final exposure with quality cuts applied is  $1.6 \cdot 10^{20}$  POT

Data quality metrics of Run 2



Data and beam quality cuts each remove  $\sim 10\%$  of POT, with small overlap such that the total loss of POT due to data and beam quality is 18.4%

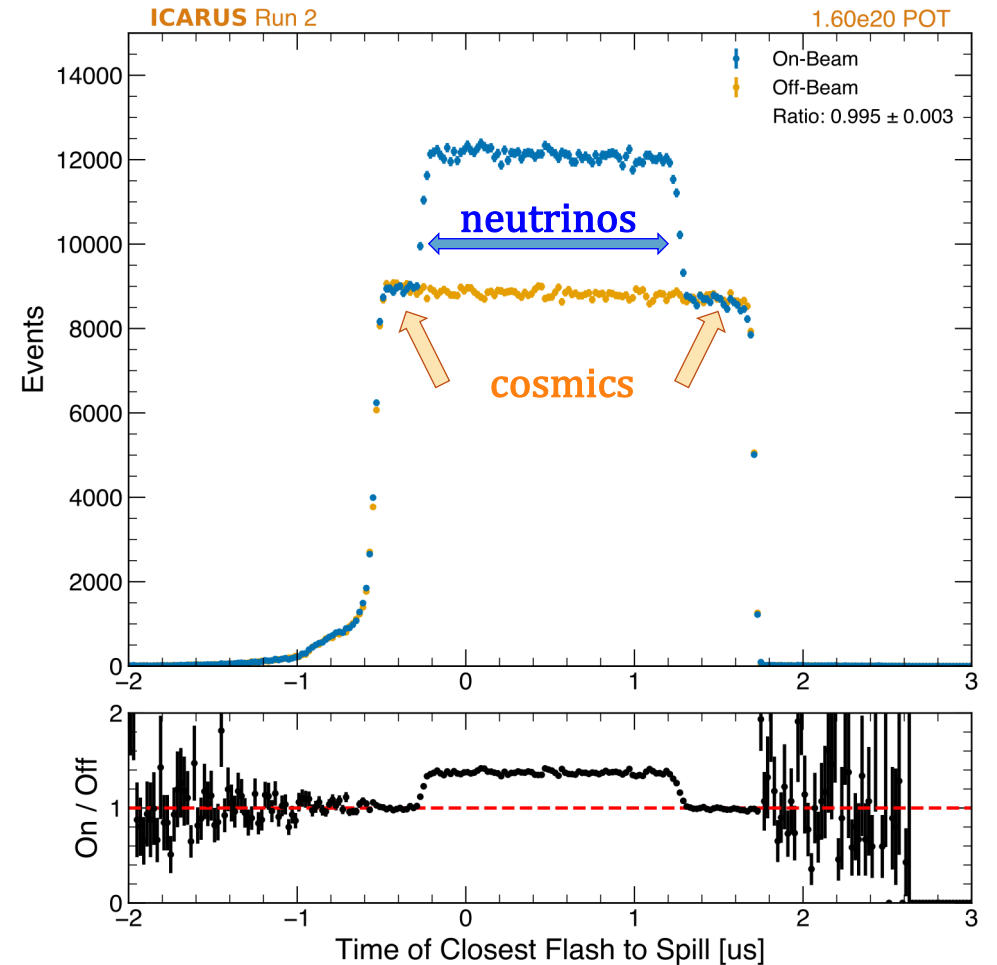
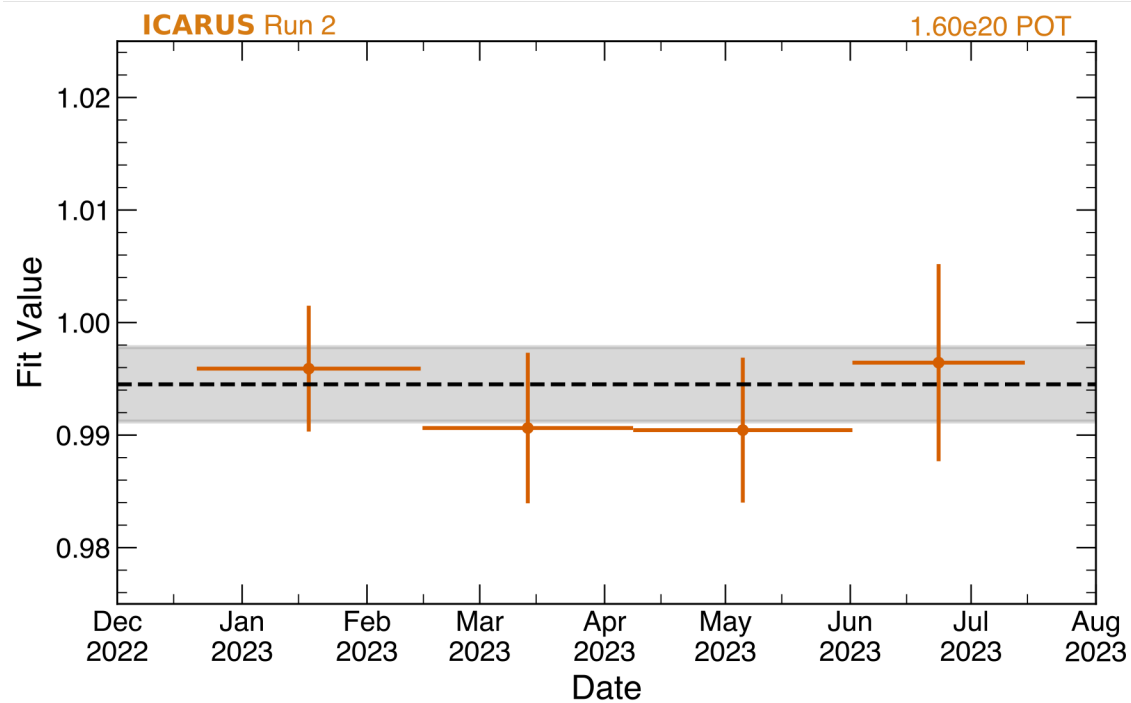
# Data and Beam quality

	POT		Spills	
	tot ( $10^{20}$ )	frac.	tot ( $10^7$ )	frac.
Total analysed	1.957	1.000	5.232	1.000
Good Runs	1.752	0.895	4.630	0.885
Beam Intensity + Horn Current	1.876	0.959	4.732	0.904
Beam Intensity + Horn Current + Good Runs	1.682	0.860	4.236	0.810
Beam Intensity + Horn Current + FoM	1.783	0.911	4.491	0.858
Beam Intensity + Horn Current + Good Runs + FoM	1.596	0.816	4.014	0.767

TABLE I: Effect of the data and beam quality conditions on the POT and spills available.

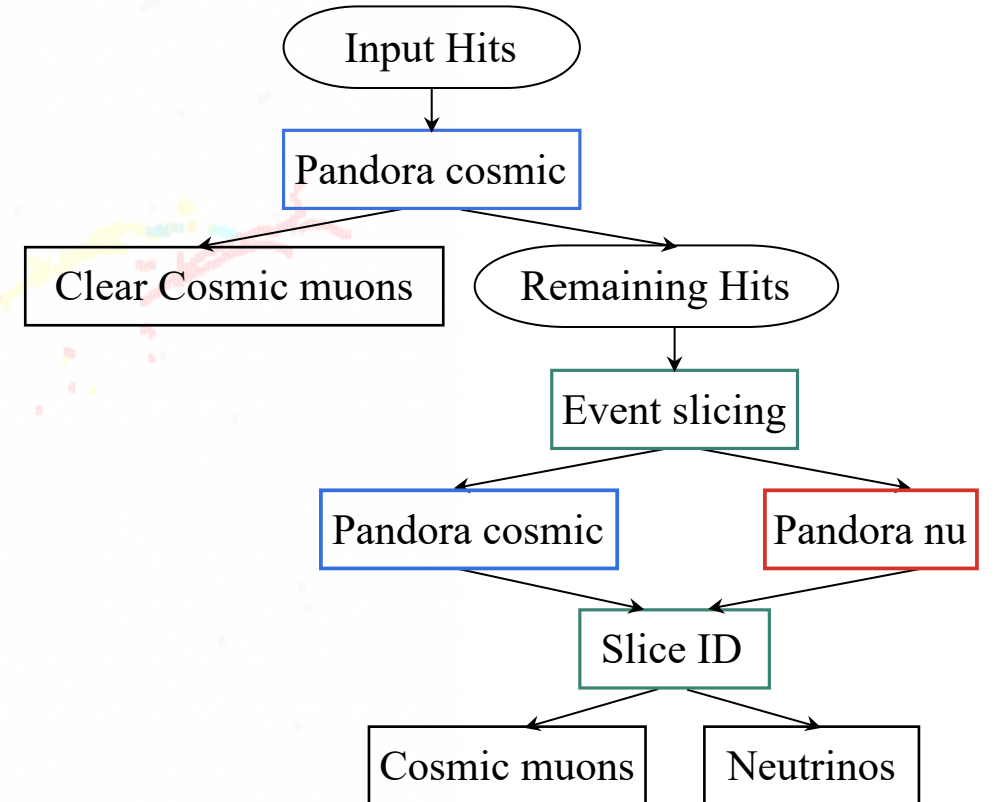
# Exposure validation

- Validation of exposure accounting performed by comparing on- and off-beam data, normalized to the same exposure, in the region of the trigger window where both streams see only cosmics
  - Observed ratio:  $0.995 \pm 0.003$ , compatible with 1
- Observed ratio consistent across the run



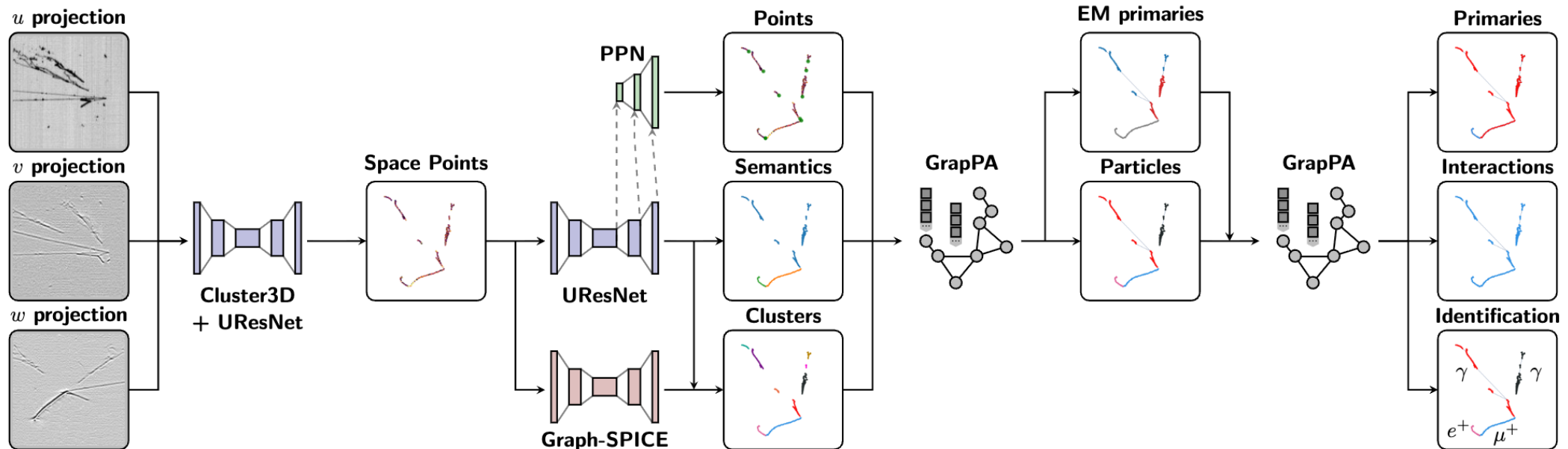
# Pandora reconstruction

- Pandora starts with raw 2D hits (single wire signals) and builds a hierarchy of tracks and showers to represent final state particles and any additional interactions or decays
- Separate paths optimized for neutrino interactions and cosmics
- Neutrino interaction path includes vertex reconstruction BDT and track/shower BDT
- PID metrics based on comparisons of  $dE/dx$  to MC templates (outside Pandora framework)



# SPINE reconstruction

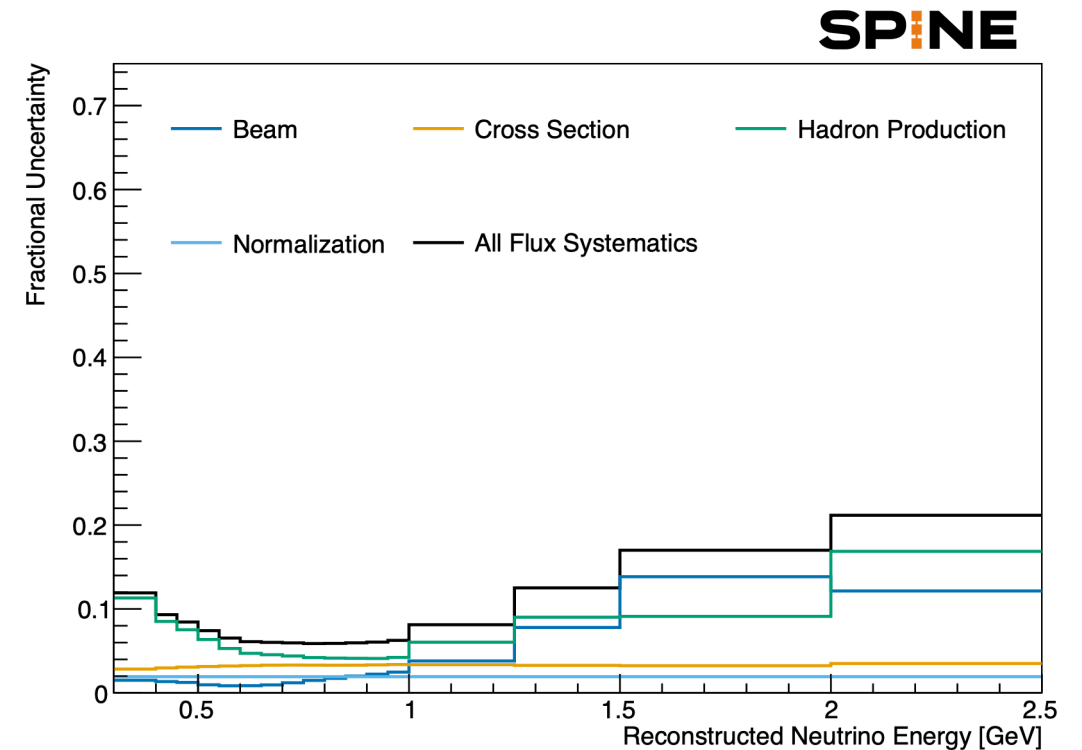
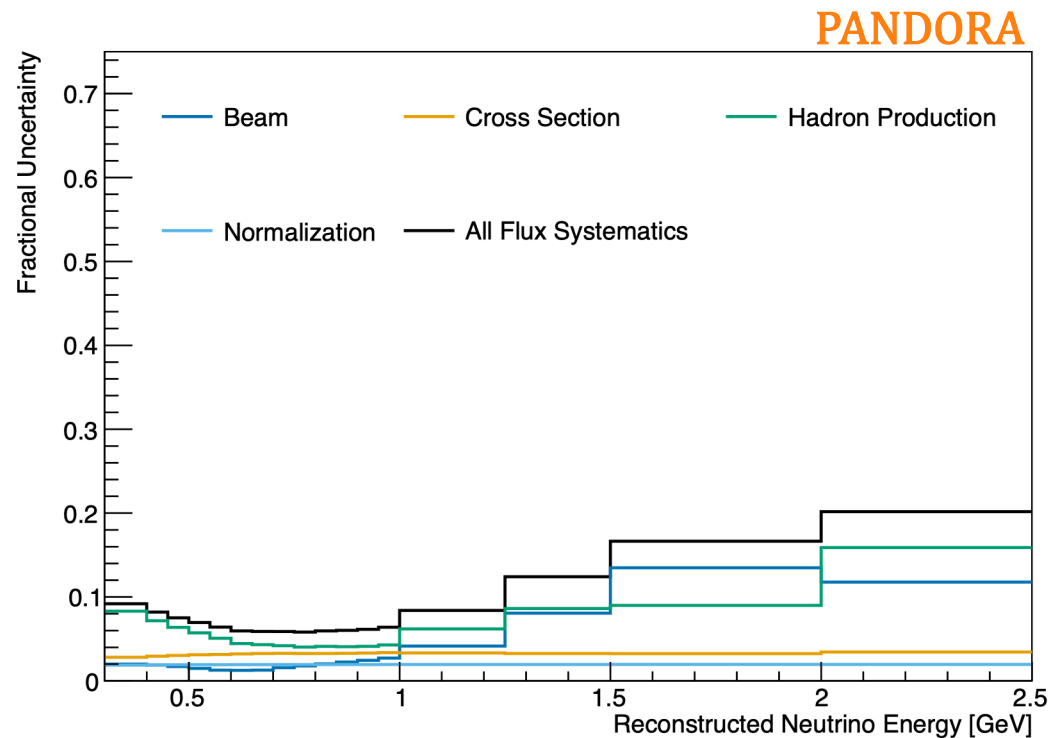
- SPINE (Scalable Particle Imaging with Neural Embeddings) uses machine learning (CNNs and GNNs) with input 3D points representing charge deposition in the detector to build high-level particle and interaction classifications → physics-driven AI
- 3D points are constructed from raw 2D hits using tomographic reconstruction
- Neural nets are trained using supervised learning techniques on physics-agnostic generators



# Systematic Uncertainties



- Full suite of systematics uncertainties. Evaluated by comparing nominal with shifted simulated samples
  - Flux model and uncertainties are the same as used by MicroBooNE and MiniBooNE [Phys. Rev. D 79 \(2009\)](#)
  - Including beam focusing,  $\sigma$  section of secondary hadronic interactions and hadron production
  - 2% overall normalization on beamline proton-on-target measurement

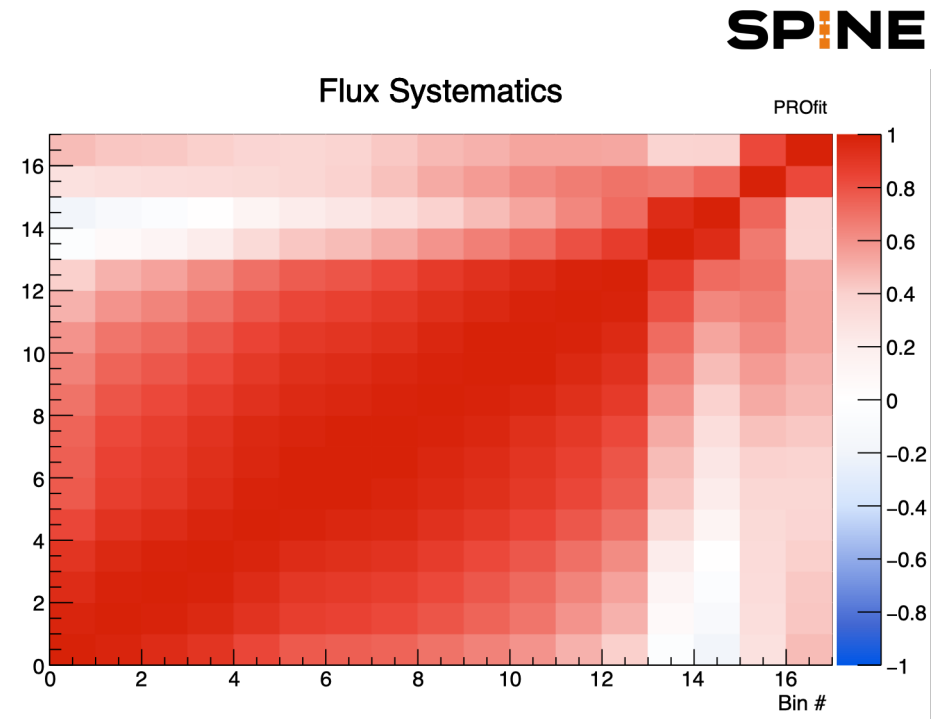
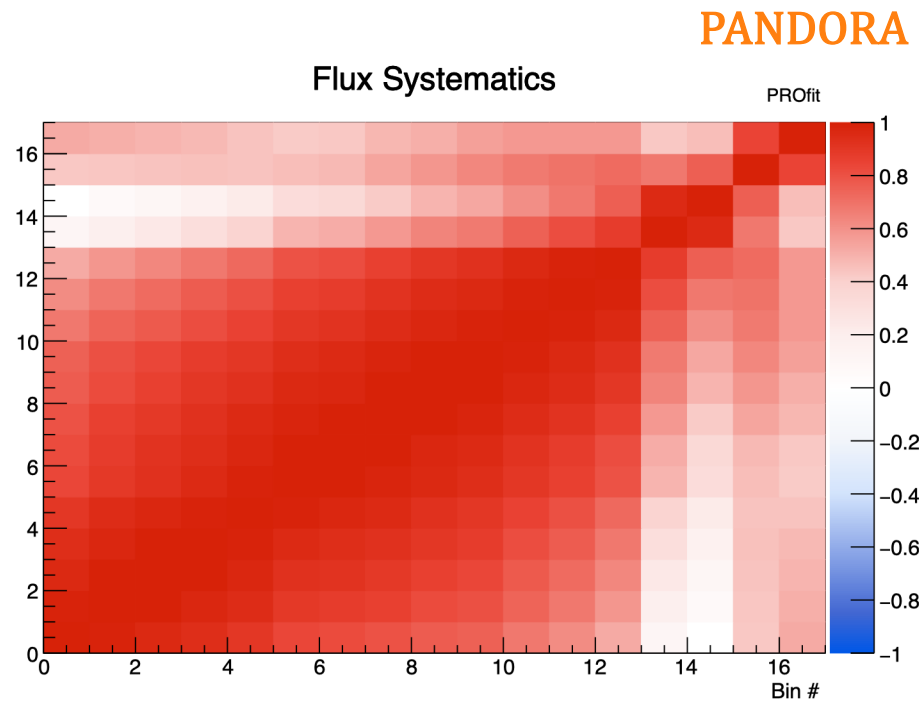


# Systematic Uncertainties



- Uncertainties are implemented as a covariance matrix generated with Monte Carlo “universes” in which the individual sources of flux uncertainty are varied randomly according to their pre-fit uncertainties

Correlation matrix in energy bins



# Systematic Uncertainties

# X-SECTION

- Interaction modeling uses GENIE AR23 (common GENIE model choice within SBN & DUNE), with nominal weights for all parameters in the CV MC
- Basic suite of systematic uncertainties and priors are taken from GENIE, with additional systematics implemented using nuSystematics
- Uncertainties are implemented using systematic weights created at generation, either using random throws to generate a covariance matrix or fitting the weights to generate splines,  $f(\sigma)$  in energy bins, each of which is associated with a nuisance parameter
  - Important uncertainties or those with non-linear response functions are treated as nuisance parameters
  - Very small contributions to the sample from NC and DIS interactions so these are all in covariance

Dial name	Short description	Central value	+1 $\sigma$	-1 $\sigma$	Implementation
ZExpB1CCQE	<i>B1</i> parameter of Z-expansion description of the axial-vector form factor on CCQE	See caption			spline
ZExpB2CCQE	<i>B2</i> parameter of Z-expansion description of the axial-vector form factor on CCQE	See caption			spline
ZExpB3CCQE	<i>B3</i> parameter of Z-expansion description of the axial-vector form factor on CCQE	See caption			spline
ZExpB4CCQE	<i>B4</i> parameter of Z-expansion description of the axial-vector form factor on CCQE	See caption			spline
RPA_CCQE	RPA suppression is turned on (off) for dial=0 (1). Dials outside [0,1] is allowed.	-	-	-	spline
CoulombCCQE	The strength of the electromagnetic potential for the Coulomb corrections on CCQE	1	20%	20%	spline
NormCCMEC	Normalization of CC-MEC	1	50%	50%	spline
NormNCMEC	Normalization of NC-MEC	1	50%	50%	covariance
XSecShape_CCMEC	dial=1 for $\nu$ and $\bar{\nu}$ distributions	-	-	-	spline
DecayAngMEC	dial=1 gives an alternative distribution proportional to $\cos^2\theta$	-	-	-	spline
FracPN_CCMEC	CC MEC proton-neutron fraction	20%	20%	20%	spline
MaCCRES	Axial-vector mass of the dipole form factor on CCRes	1.088962	20%	20%	spline
MvCCRES	Vector mass of the dipole form factor on CCRes	0.840	10%	10%	spline
MaNCRES	Axial-vector mass of the dipole form factor on NCRes	1.088962	20%	20%	covariance
MvNCRES	Vector mass of the dipole form factor on NCRes	0.840	10%	10%	covariance
NonRESBGvpNC1pi	Scale factor for the non-resonance background level ( $W < 2\text{GeV}c^2$ ) of $\nu$ -p NC + $1\pi$	1	50%	50%	covariance
NonRESBGvpNC2pi	Scale factor for the non-resonance background level ( $W < 2\text{GeV}c^2$ ) of $\nu$ -p NC + $2\pi$	1	50%	50%	covariance
NonRESBGvpNC1pi	Scale factor for the non-resonance background level ( $W < 2\text{GeV}c^2$ ) of $\bar{\nu}$ -p NC + $1\pi$	1	50%	50%	covariance
NonRESBGvpNC2pi	Scale factor for the non-resonance background level ( $W < 2\text{GeV}c^2$ ) of $\bar{\nu}$ -p NC + $2\pi$	1	50%	50%	covariance
NonRESBGvnNC1pi	Scale factor for the non-resonance background level ( $W < 2\text{GeV}c^2$ ) of $\nu$ -n NC + $1\pi$	1	50%	50%	covariance
NonRESBGvnNC2pi	Scale factor for the non-resonance background level ( $W < 2\text{GeV}c^2$ ) of $\nu$ -n NC + $2\pi$	1	50%	50%	covariance
NonRESBGvnNC1pi	Scale factor for the non-resonance background level ( $W < 2\text{GeV}c^2$ ) of $\bar{\nu}$ -n NC + $1\pi$	1	50%	50%	covariance
NonRESBGvnNC2pi	Scale factor for the non-resonance background level ( $W < 2\text{GeV}c^2$ ) of $\bar{\nu}$ -n NC + $2\pi$	1	50%	50%	covariance
NonRESBGvbarpNC1pi	Scale factor for the non-resonance background level ( $W < 2\text{GeV}c^2$ ) of $\bar{\nu}$ -p NC + $1\pi$	1	50%	50%	covariance
NonRESBGvbarpNC2pi	Scale factor for the non-resonance background level ( $W < 2\text{GeV}c^2$ ) of $\bar{\nu}$ -p NC + $2\pi$	1	50%	50%	covariance
NonRESBGvbarpNC1pi	Scale factor for the non-resonance background level ( $W < 2\text{GeV}c^2$ ) of $\bar{\nu}$ -p NC + $1\pi$	1	50%	50%	covariance
NonRESBGvbarpNC2pi	Scale factor for the non-resonance background level ( $W < 2\text{GeV}c^2$ ) of $\bar{\nu}$ -p NC + $2\pi$	1	50%	50%	covariance
NonRESBGvbarncNC1pi	Scale factor for the non-resonance background level ( $W < 2\text{GeV}c^2$ ) of $\bar{\nu}$ -n NC + $1\pi$	1	50%	50%	covariance
NonRESBGvbarncNC2pi	Scale factor for the non-resonance background level ( $W < 2\text{GeV}c^2$ ) of $\bar{\nu}$ -n NC + $2\pi$	1	50%	50%	covariance
AhtBY	$A_{HT}$ higher twist parameter in BY model scaling $\xi_W$	0.538	25%	25%	covariance
BhtBY	$B_{HT}$ higher twist parameter in BY model scaling $\xi_W$	0.305	25%	25%	covariance
CV1uBY	$C_{\nu 1u}$ u valence GRV08 PDF correction parameter in BY model	0.291	30%	30%	covariance
CV2uBY	$C_{\nu 2u}$ u valence GRV08 PDF correction parameter in BY model	0.189	40%	40%	covariance
NormCCCOH	Normalization of CC-COH	1	100%	100%	covariance
NormNCCOH	Normalization of NC-COH	1	100%	100%	covariance
MFP_pi	Scale factor for the mean free path in the FSI of $\pi$	1	20%	20%	covariance
FrCEX_pi	Scale factor for the fraction of charge-exchange fate in the FSI of $\pi$	1	50%	50%	spline
FrInel_pi	Scale factor for the fraction of inelastic scattered fate in the FSI of $\pi$	1	40%	40%	covariance
FrAbs_pi	Scale factor for the fraction of absorption fate in the FSI of $\pi$	1	30%	30%	covariance
FrPiProd_pi	Scale factor for the fraction of pion production fate in the FSI of $\pi$	1	20%	20%	covariance
MFP_N	Scale factor for the mean free path in the FSI of nucleon	1	20%	20%	covariance
FrCEX_N	Scale factor for the fraction of charge-exchange fate in the FSI of nucleon	1	50%	50%	spline
FrInel_N	Scale factor for the fraction of inelastic scattered fate in the FSI of nucleon	1	40%	40%	covariance
FrAbs_N	Scale factor for the fraction of absorption fate in the FSI of nucleon	1	20%	20%	covariance
FrPiProd_N	Scale factor for the fraction of pion production fate in the FSI of nucleon	1	20%	20%	covariance
MaNCEL	Axial-vector mass of the dipole form factor on NCEL	0.994989	25%	25%	covariance
EtaNCEL	Strange axial-vector mass of the dipole form factor on NCEL	0.12	30%	30%	covariance

Quasi-elastic

Meson Exchange Current

Resonance

Non-Resonance BG

Deep Inelastic Scattering

Coherent

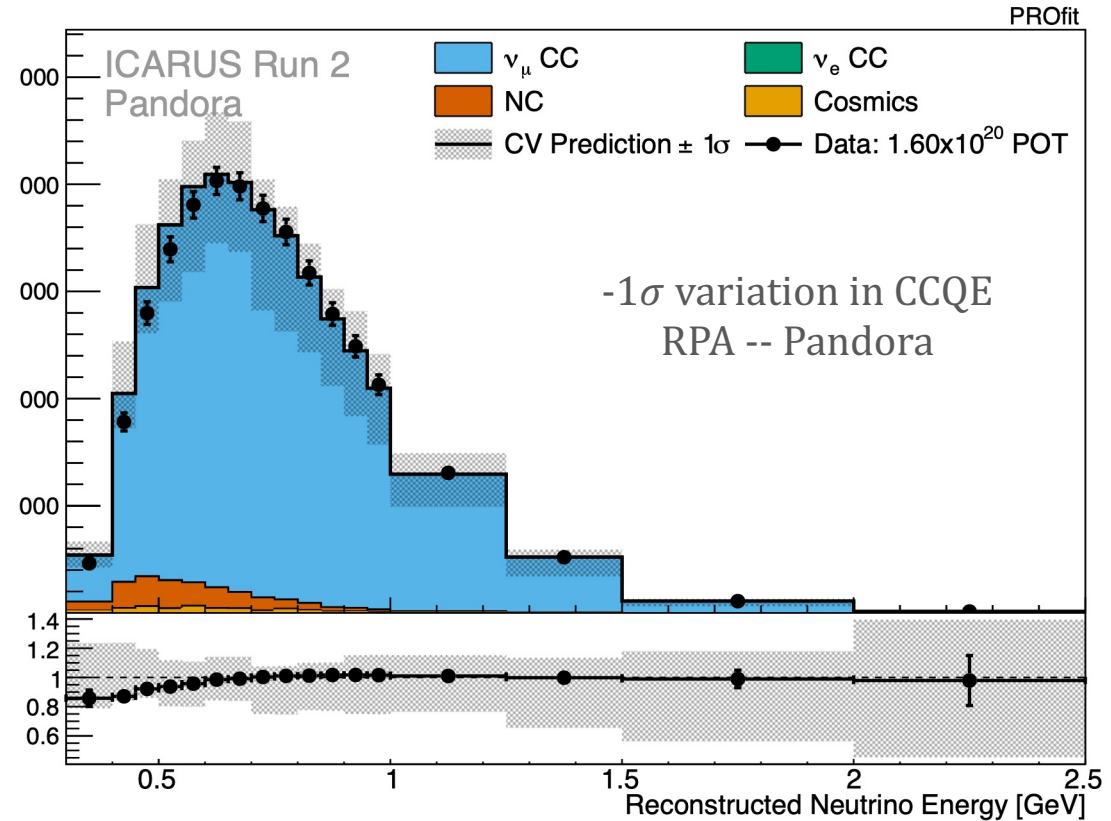
Final State Interactions

Neutral Current

# Systematic Uncertainties

- CC QE parameters:
  - Z-expansion description of the axial form factor
  - RPA suppression: largest systematic impact for lowest energy bins
  - Coulomb correction strength
- CC MEC
  - Normalization: largest systematic impact for medium to high energy bins
  - Reweight to Valencia model
  - Alternative decay angle distribution
  - pn and nn initial state fractions
- CC RES: axial and vector masses
- FSI: pion and nucleon charge exchange

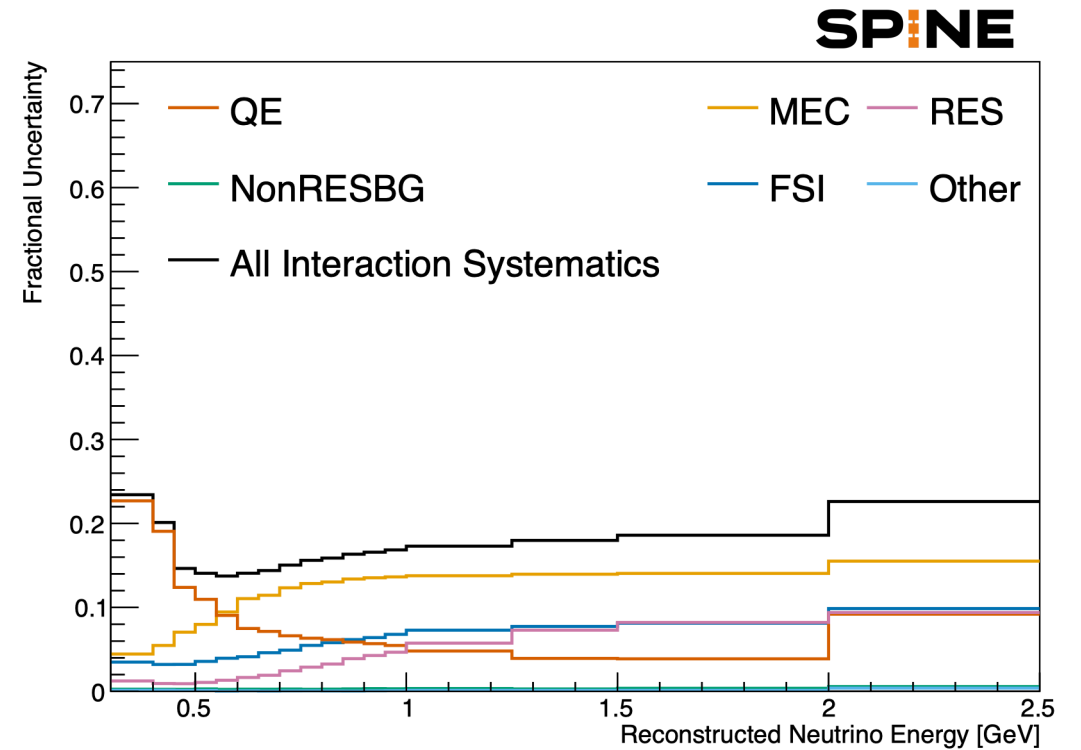
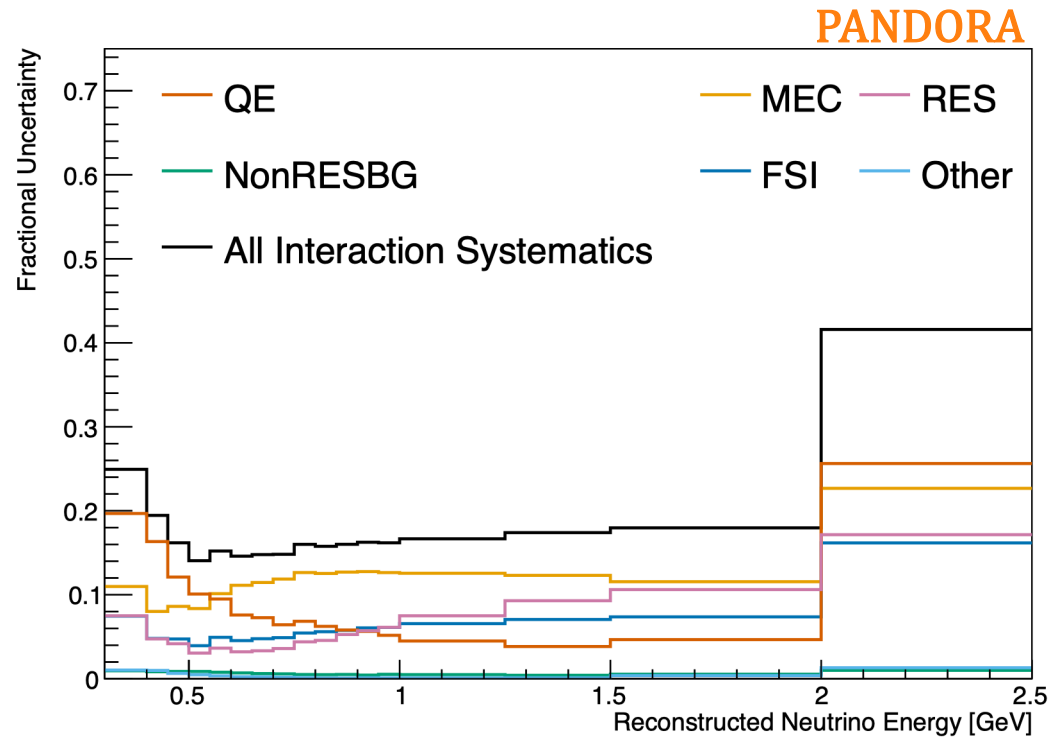
## X-SECTION



# Systematic Uncertainties

# X-SECTION

- Interaction model fractional uncertainty



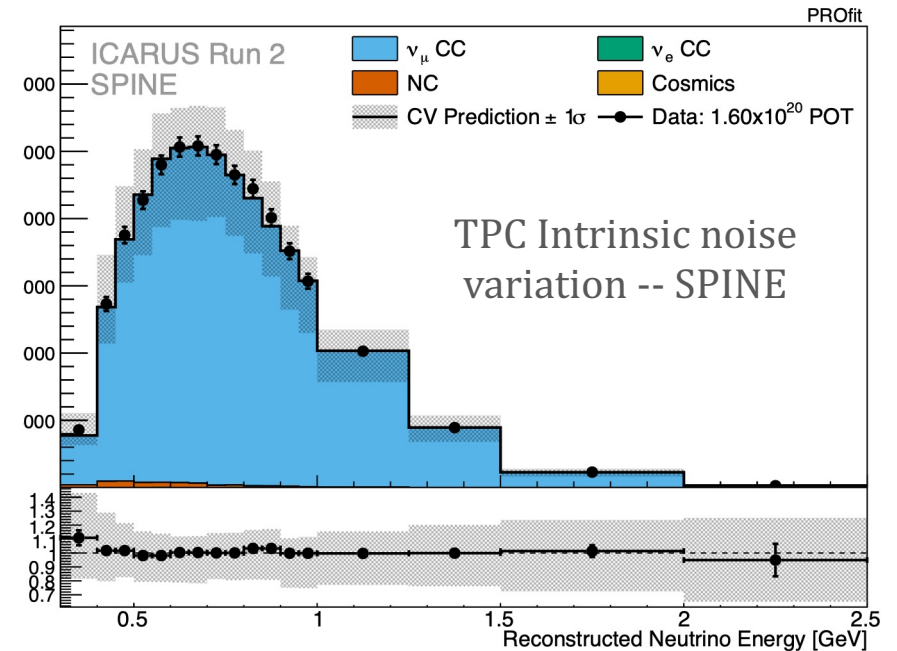
# Systematic Uncertainties

# DETECTOR

- Detector systematics are evaluated by a “brute force MC” method, using ratio of selected events in an alternative MC model to the CV MC as weights included in the fit as nuisance parameters
  - Note that this procedure allows us to limit the size of a possible effect from each systematic but is limited by the MC statistics in our variation samples

- Most significant systematic variations:

- Unmodeled channel-to-channel intrinsic noise variations
- Unmodeled variations in TPC signal shape
- Unmodeled spatial non-uniformity in detector response
- Alternative model of recombination
- Variation of electron lifetime (closer to true value)

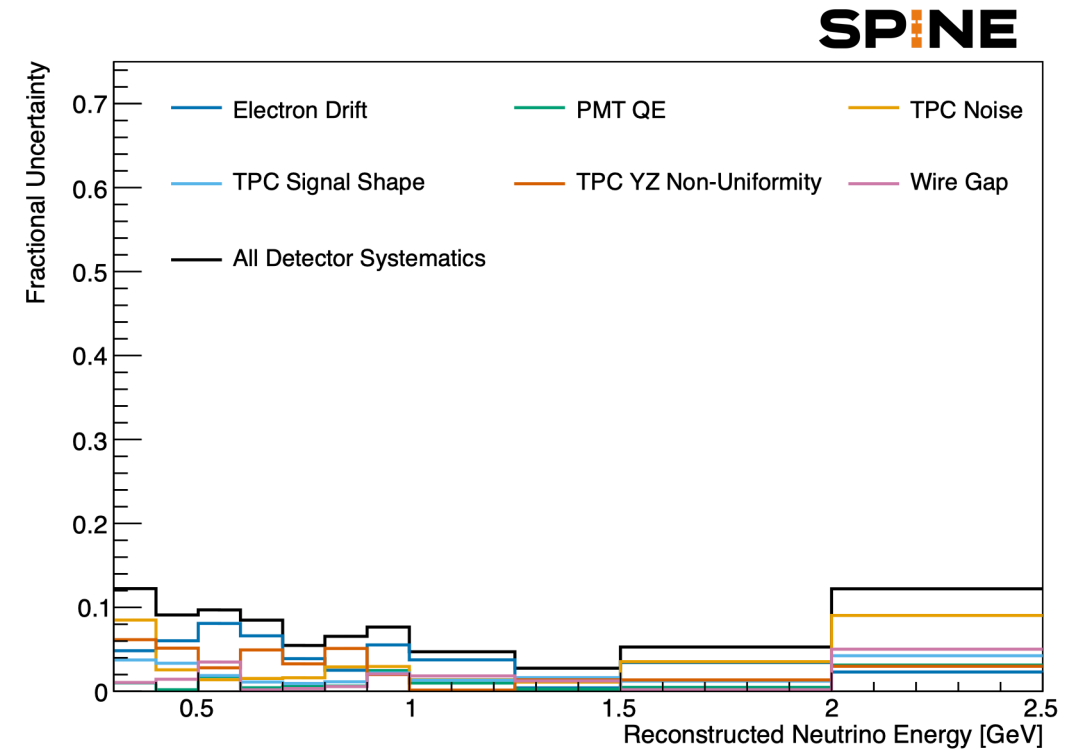
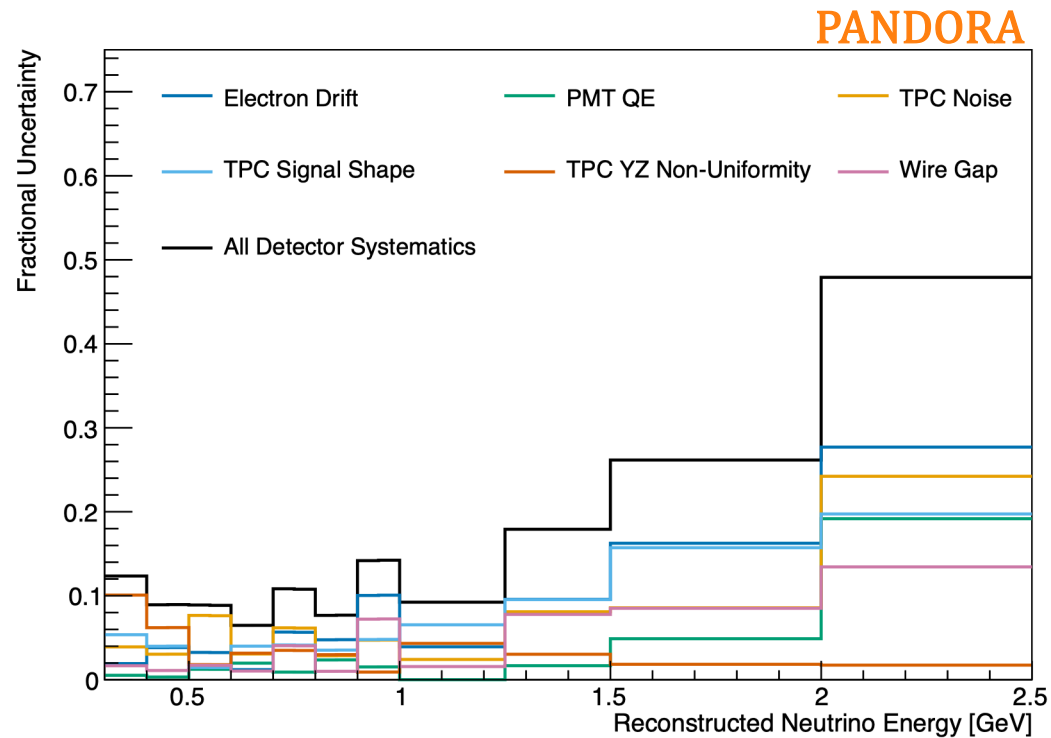


Also considered: variations in TPC coherent noise, variations in scintillation light yield, unmodeled gap in the induction 1 wire plane, unmodeled cathode non-planarity, uncertainty in trigger efficiency, variations of fiducial volume and containment cuts

# Systematic Uncertainties

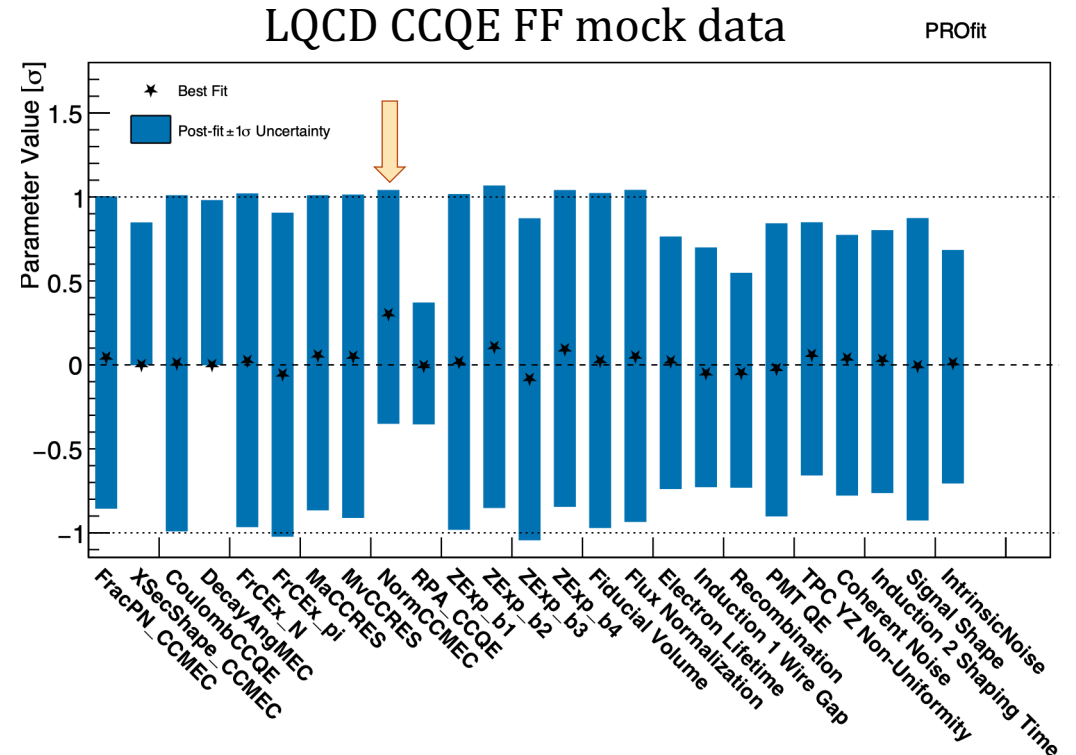
# DETECTOR

- Detector model fractional uncertainty



# Mock data studies

- Generate mock data with alternative model and fit against CV MC as a test of systematics model
  - Injected oscillation signal
  - Alternative interaction models: FSI, CCQE form factor, MEC model
  - Reweight to other generators in leading proton kinematic variables (NUISANCE): NEUT, NuWro, GiBUU
  - “Nightmare scenario” where systematic parameter values are cherry-picked to mimic an oscillation
  - Artificial variation of CCNp component to study impact of particle-detector interaction (G4) uncertainties
- **Injected oscillation signals were recovered, and no false signals or extreme pulls were observed in any of the mock data fits**



The fitter prefers to distribute the variation over several  $<1\sigma$  pulls rather than attributing it all to one large variation and the systematic parameter being pulled does not always correspond exactly to the physics being varied. (eg: CC MEC normalization)

# Results: nuisance parameters

- No nuisance parameters pulled beyond  $\sim 1\sigma$
- Pull on CC MEC normalization is to compensate for normalization mismatch between data and CV MC
- RPA constraint is also likely a normalization effect
- Pull on recombination is not consistent with expectation from known detector parameters and thus is likely degenerate with some other effect present in the data

